EFFECTS OF MANIPULATOR RESTRAINTS ON HUMAN OPERATOR PERFORMANCE

R. E. Magdaleno
D. T. McRuer

FOREWORD

This report documents a portion of an analytical and experimental investigation of human pilot dynamics accomplished under Contract No. AF 33(657)-10835, BPS No. 5(6399-8219-62405364), sponsored by the Flight Control Division of the Air Force Flight Dynamics Laboratory. On a predecessor project, Contract AF 33(616)-7501, Project No. 8219, Task No. 821905, a comprehensive report entitled Human Pilot Dynamics in Compensatory Systems: Theory, Models, and Experiments with Controlled Element and Forcing Function Variations, AFFDL-TR-65-15, July 1965, thoroughly documents the description of the pilot-vehicle closed loop system and forms the basis for the present efforts.

The research was performed by Systems Technology, Inc., Hawthorne, California, and under subcontract by the Franklin Institute Laboratories for Research and Development, Philadelphia, Pennsylvania. The project principal investigators were D. T. McRuer and Dunstan Graham of STI and E. S. Krendel of FIL. The Flight Control Division project engineers were Capt. J. E. Pruner and P. E. Pietrzak.

The major contributors besides the authors and the principal investigators were William Reisener, Jr., in experimental planning and execution and R. J. Wasicko in experimental planning. An indispensable portion of the program, the design and development of analysis apparatus, was accomplished on the predecessor project by R. A. Peters and K. A. Ferrick. The authors would like to thank M. M. Solow of FIL for his dedicated effort as the experimental subject and Diana Fackenthal of FIL for her diligence in data reduction. Finally, the many review comments and suggestions by R. O. Anderson, P. E. Pietrzak, G. G. Frost and R. J. Woodcock have significantly improved the report.

The contractor's internal report number was STI-TR-134-2. This manuscript was released by the authors in December 1966 for publication as an RTD Technical Report.

This technical report has been reviewed and is approved.

C. B. WESTBROOK
Chief, Control Criteria Branch
Flight Control Division
AF Flight Dynamics Laboratory

ABSTRACT

This report is concerned with a series of experiments in which the effects of manipulator restraints, i.e., load dynamics imposed on the pilot, are central. The purposes of this investigation are to:

- Determine the load effects on the pilot's describing functions and performance measures for a representative variety of manipulator restraints and controlled elements
- Provide inferential insight into the relative importance of limb position and output force senses in manual control.

The results indicate that the pilot performs best with a spring restrained manipulator. With pure inertia restraint there is a large performance degradation unless the inertia is less than that given by the pilot's output limb acting on the manipulator. Generally, the pilot has good position feedback in that his describing function form is essentially invariant to a wide range of spring and inertia restraints for the same controlled element.

TABLE OF CONTENTS

ILLUSTRATIONS

TABLES

SYMBOLS

a_T	Threshold value of the indifference threshold nonlinearity
A	Muscle actuation signal
b_a	Effective damping of limb output system
b_s	Manipulator damping
B5, B6	Forcing function designation defined on page 19
c(t)	Limb position
e(t)	Error time function
F(t), F_L	Limb-applied force
F_M	Force on manipulator
F_E	External force
G_{A_1}, G_{A_2}	Actuation elements
G_e	Eye dynamics, central computational delays, equalization and gain adjustment, synaptic and conduction delays to spinal centers involved, etc.
G_{F_1}	Command feedforward
G_K	Force feedback elements
G_L	Load characteristics of output member and manipulator
G_M	Load characteristics of manipulator
G_P	Position feedback elements
i(t)	Forcing function time function
I_a	Effective inertia of limb
I_{max}	Maximum inertia of manipulator
I_{min} or I_m	Minimum inertia of manipulator
I_s	Manipulator inertia
I_1	Specific value of manipulator inertia (page 19)

k	Manipulator spring rate
k_a	Effective spring rate of limb output system
k_c	Spring rate for clamped manipulator
k_s	Manipulator spring rate
K_a	Position control sensitivity (defined on page 18)
K_c	Controlled element gain
K_{F_1}, K_{F_a}	Force control sensitivity (defined on page 18)
K_p	Human pilot gain
K_T	Gain of indifference threshold describing function
K_1	Position control sensitivity (defined on page 18)
$m(t)$	System output time function
RO.40	Forcing function designation defined on page 19
T	Time constant
T_I	General lag time constant of human pilot describing function
T_K, T_K'	Lead and lag time constants in precision model of human pilot describing function
T_L	General lead time constant of human pilot describing function
$T_{L_{hi}}$	General lead time constant of human pilot describing function when it is a small quantity
T_N	First-order lag time constant approximation of the neuromuscular system
T_{N_1}	First-order lag time constant of the neuromuscular system
Y_c	Controlled element (machine and display) transfer function
Y_p	Pilot describing function
α	Low frequency phase approximation parameter
δ	Stick position
ζ_N	Damping ratio of second-order component of the neuromuscular system

θ_i	Neuromuscular System Command
σ_e	Standard deviation of error signal, e(t)
σ_i	rms value of the forcing function
σ_T	rms value of input to the indifference threshold
τ	Pure time delay
τ_e	Effective time delay
$\Phi_{i\delta}$	Cross power spectral density between i and δ
Φ_{iF_L}	Cross power spectral density between i and F_L
ω	Angular frequency, rad/sec
ω_c	System crossover frequency, i.e., frequency at which $\lvert Y_p Y_c \rvert = 1$
ω_i	Forcing function bandwidth
ω_N	Undamped natural frequency of second-order part of the neuromuscular system
$\doteq$	Approximately equal to
$\measuredangle$	Angle of
db	Decibels; $10 \log_{10}$ ( ) if a power quantity, e.g., spectrum; $20 \log_{10}$ ( ) if an amplitude quantity, e.g., Y_p
$\lvert\ \rvert$	Magnitude
$\lvert\ \rvert_{db}$	Magnitude in db
"	Inches
$\uparrow$	Increase
$\downarrow$	Decrease

SECTION I

INTRODUCTION

Within the last decade there has been a number of experimental programs aimed at finding the random-input describing function of the human operator in compensatory situations, Refs. 1, 2, and 3. This general control situation is illustrated in Fig. 1. The key task variables represented there are the manipulator load dynamics, the forcing function, and the controlled element characteristics. Most of the past work on human operator dynamics has been concerned with the effects of controlled element and forcing function. A comprehensive experimental and analytical study of human pilot dynamics has recently been completed by the Systems Technology-Franklin Institute team under U. S. Air Force Flight Dynamics Laboratory sponsorship. In the most extensive experimental series in this program (Ref. 1) the manipulator was eliminated as a task variable by using the same spring-restrained sidestick for a wide variety of controlled element and input bandwidth combinations. In another series (Ref. 8) the manipulator was an important experimental variable. There, limiting cases of a free-moving controller and a pressure (strain gauge) controller were used in addition to the spring-restrained sidestick.

This report is concerned with a third series of experiments in which the effects of manipulator restraints, i.e., load dynamics imposed on the operator, are central. The purposes of this investigation are to:

a. Determine the load effects on human operator describing functions for a representative variety of manipulator restraints and controlled elements

b. Provide inferential insight into the relative importance of limb position and output force senses in manual control.

These data and insights are needed to improve our understanding of two types of vehicle handling qualities and man-machine system problems:

a. The effects of manipulators on pilot dynamic responses and overall pilot-vehicle system performance. These

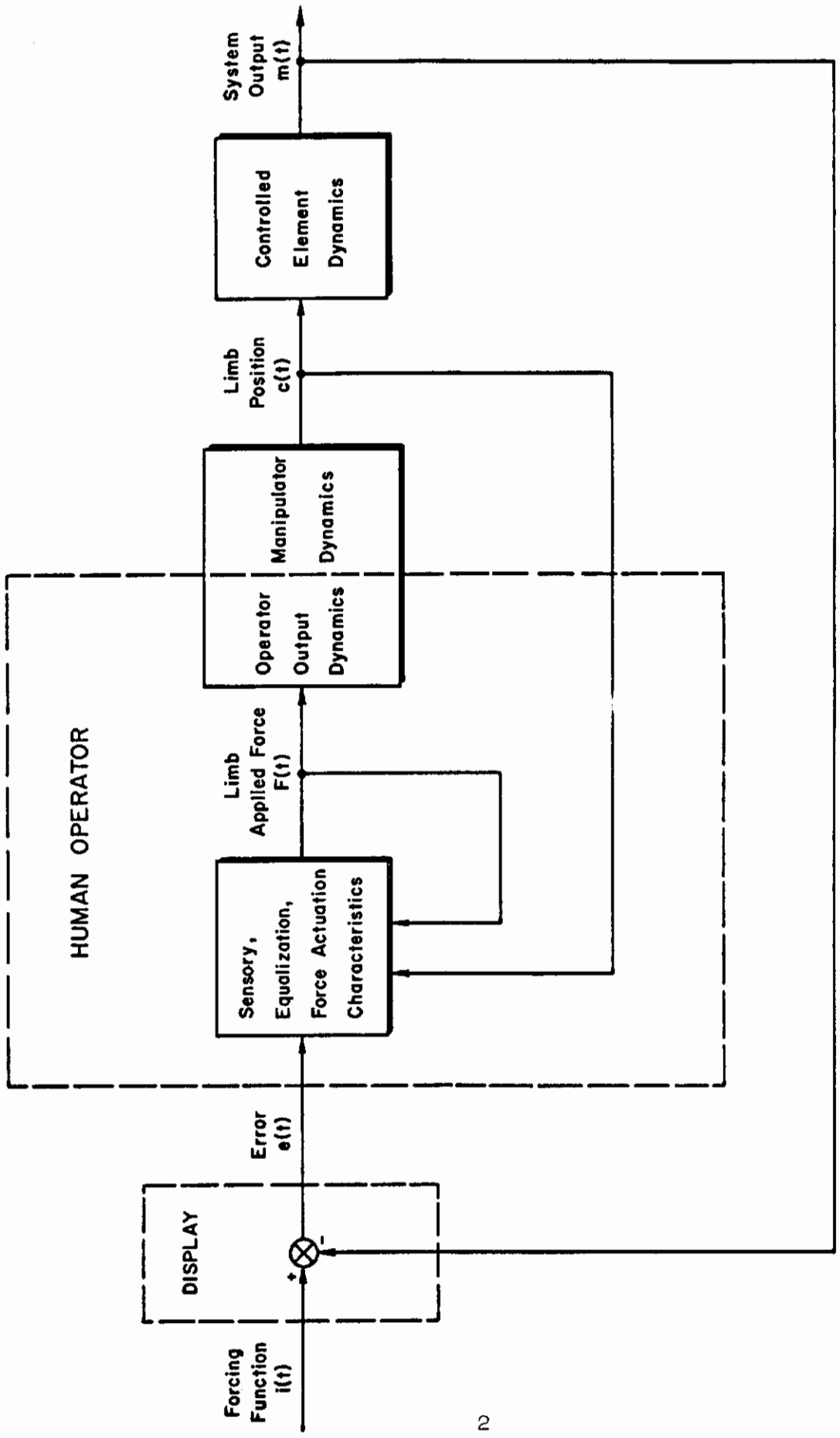

Figure 1. Single-Loop Manual Control System

relate both to manipulator types (wheel, center stick, side-stick, etc.) and to manipulator functional (force-displacement) characteristics.

b. The likely effects of control system nonlinearities (e.g., hysteresis, backlash, coulomb friction, preload) on pilot-vehicle system stability. Practically, this should lead to a better understanding of some kinds of pilot induced oscillations, and to the establishment of necessary or sufficient conditions for their elimination.

The detailed experimental plan for the various configurations to be tested will be considered after a summary of previous works relating to manipulator restraints. The Pre-Experimental Analysis of Section II further sharpens and delineates desirable experiments.

A. SUMMARY OF EARLIER EXPERIMENTS PERFORMED BY SYSTEMS TECHNOLOGY-FRANKLIN INSTITUTE

1. Effects of Forcing Function and Controlled Element Variations on Describing Function Models (Ref. 1)

The extensive experimental series mentioned earlier (Ref. 1) yielded an excellent data base for modeling the overall human operator describing function, and to a certain extent the various subsystems involved. For some configurations, the data were of such low variability that the following relatively complex model form was the minimum necessary to yield an adequate fit.

$$Y_p \doteq K_p K_T \left(\frac{a_T}{\sigma_T}\right)\left(\frac{T_L j\omega + 1}{T_I j\omega + 1}\right)\underbrace{\left(\frac{T_K j\omega + 1}{T_K' j\omega + 1}\right)}_{\doteq e^{-j\alpha/\omega}}\underbrace{\frac{1}{\left(T_{N_1} j\omega + 1\right)\left[\left(\frac{j\omega}{\omega_N}\right)^2 + \frac{2\zeta_N j\omega}{\omega_N} + 1\right]}}_{\doteq 1/\left(T_N j\omega + 1\right) \quad \text{or } e^{-j\omega T_N}} e^{-j\omega\tau} \qquad (1)$$

neuromuscular system terms

where

K_p = gain

$K_T\left(\frac{a_T}{\sigma_T}\right)$ = indifference threshold describing function $\left[1 - (a_T/\sigma_T)\sqrt{2/\pi}\right.$ when $a_T/\sigma_T \ll 1$]

$\frac{T_L j\omega + 1}{T_I j\omega + 1}$ = equalization characteristic, T_L and T_I values depend on form of controlled element

τ = fixed time delay due to conduction times of the various subsystem elements

$\frac{T_K j\omega + 1}{T'_K j\omega + 1}$ = low frequency terms which are used to describe low frequency phase data often approximated by $e^{-j(\alpha/\omega)}$ for $\omega > 1/T_K$ or $1/T'_K$

$\frac{1}{\left(T_{N_1} j\omega + 1\right)\left[\left(\frac{j\omega}{\omega_N}\right)^2 + \frac{2\zeta_N j\omega}{\omega_N} + 1\right]}$ = neuromuscular system terms often approximated by $1/(T_N j\omega + 1)$ or $e^{-j\omega T_N}$

Equation 1 is the most refined version of the pilot model discussed in Ref. 1. The low frequency terms approximated by $e^{-j(\alpha/\omega)}$ are new, i.e., the data trends supporting them had appeared before (Refs. 2 and 5), but were ignored due to suspected analyzer inaccuracies.

The third-order neuromuscular system elements are compatible with known characteristics, i.e., the second-order term is representative of the spring-mass system of the limb, while the first-order term is a simple approximation to actuation lags. These terms are also compatible with some aspects of transient responses (Ref. 5).

For many controlled elements an acceptable approximation to Eq. 1 over a restricted but fairly wide frequency range is

$$Y_p \doteq K_p\left(\frac{T_L j\omega + 1}{T_I j\omega + 1}\right) e^{-j\left[(\tau + T_N)\omega + \frac{\alpha}{\omega}\right]} \qquad (2)$$

The values of T_L and T_I depend on the controlled element. In general, the human operator selects them such that the magnitude of the open-loop system, Y_pY_c, has approximately a −20 db/decade slope in the region of crossover. The details of the pilot adjustment rules, Ref. 1, are beyond the scope of this discussion. With the proper selection of T_L and T_I, the open-loop system can be described by

$$Y_pY_c \doteq \frac{\omega_c e^{-j(\tau_e\omega + \frac{\alpha}{\omega})}}{j\omega} \tag{3}$$

where

$$\tau_e = \tau + T_N - T_{L_{hi}}$$

$$T_{L_{hi}} = T_L \text{ when it is available at high frequency}$$

The lead time constant, T_L, can be used to reduce the effective time delay, τ_e, when this lead term has not been required at low frequency to yield the −20 db per decade slope of the open-loop system. Specifically for $Y_c = K_e/s^2$ the lead term is required at low frequency and therefore is not available for reducing the effective time delay, τ_e.

2. Various Manipulators Experiments (Ref. 8)

The various manipulators experiments used three manipulator types (pressure, free-moving, and spring-restrained controls) three controlled elements and two input bandwidths. The pressure (strain gauge) control is at one extreme (essentially infinite spring) while the free-moving control had no restraint except its own very small inertia. The spring-restrained control is between these extremes. These manipulators were used in a lateral control task in which the displayed error moved horizontally.

The basic result of this series of experiments was that the pressure control had significantly less phase lag at high frequencies and the same or less phase lag at low frequencies compared to the free-moving control

(the spring-restrained control was intermediate). Further, the normalized mean-squared error was ordinarily smallest for the pressure control.

B. MATHEMATICALLY EQUIVALENT TRACKING SYSTEMS

Reference 4 investigated the effects on mean square error of dynamics in the loop as electronic controlled elements and/or as mechanical restraints. The basic hypothesis was that human tracking performance would remain unchanged despite variations in mechanical restraints if the overall transfer function from control force to visual display was unchanged. In effect, this was an attempt to assess the importance of the position feedbacks.

The experiments were organized in three phases. The first used a spring-centered control stick with inertia, damping, and spring rate variable and $Y_c = K_c$. The second phase utilized a pressure stick plus controlled element dynamics identical to each of the force-displacement relationships used in the first phase. The third phase used a free-moving control similar to that in the various manipulators experiments mentioned earlier, although a very light spring restraint was added. The controlled element had the same form as in the other phases. Thus, phases one and two provided a comparison of control dynamics as mechanical restraints or as electronic controlled elements. Phases two and three provided the same type of comparison between a pressure control and a free-moving control similar to that discussed in the various manipulator experiments. Phases two and three included some additional experiments in which the controlled element was $Y_c = K_c$. These latter experiments afforded a comparison among the three manipulator types similar to the various manipulator experiments in the previous section.

The best results with each of the three manipulator types (phase one with very small inertia) and $Y_c = K_c$ show that the pressure control gave slightly less mean square error although all three were less than 1 db apart. Comparison of phase one with phase two showed that mean square error with mechanical restraints was significantly larger than with their electronic analogs. One possible explanation is that the human operator does utilize motor feedback to improve control although an alternate possibility does exist, viz., the human operator has a series equalization

capability, Ref. 1, p. 185, which could well explain the differences between the two experiments. The verification of the hypothesis stated in Ref. 4 will require describing function measurements in addition to performance measures.

C. IMPLICATIONS OF THE REVIEW OF RECENT EXPERIMENTS

Current interpretations of the experiments discussed in Section A above go a long way toward providing a data base for the development of a mathematical description of the neuromuscular system. But this data base is confined to experiments with variations of controlled element, forcing function, and, to a certain extent, manipulator restraints. As a minimum the review in Sections A and B above indicates a need to investigate inertia effects and the interchange of dynamics due to mechanical restraints with those due to electronic controlled elements. This last point could be restated as: To what extent can the human act as a force output or a position output device? These, plus other interesting experiments, will be brought into sharper focus by the pre-experimental analysis to follow.

SECTION II

PRE-EXPERIMENT ANALYSIS

The purpose of this section is to investigate the implications of the neuromuscular system model on describing function measurements. As will be shown, the human operator can be described by a number of serially connected describing function boxes such that no one experiment can isolate the effects due to a particular box. A series of experiments is needed of which some are critical with respect to the question of the human operator being a force or position output device.

A. EXPERIMENTAL CONFIGURATION

As shown in the block diagram of Fig. 2, the variable-restraint experimental apparatus is configured so that a signal proportional to either the position of or force on the manipulator can be used to drive the controlled element. Limiting cases of free-moving and pressure manipulators have been

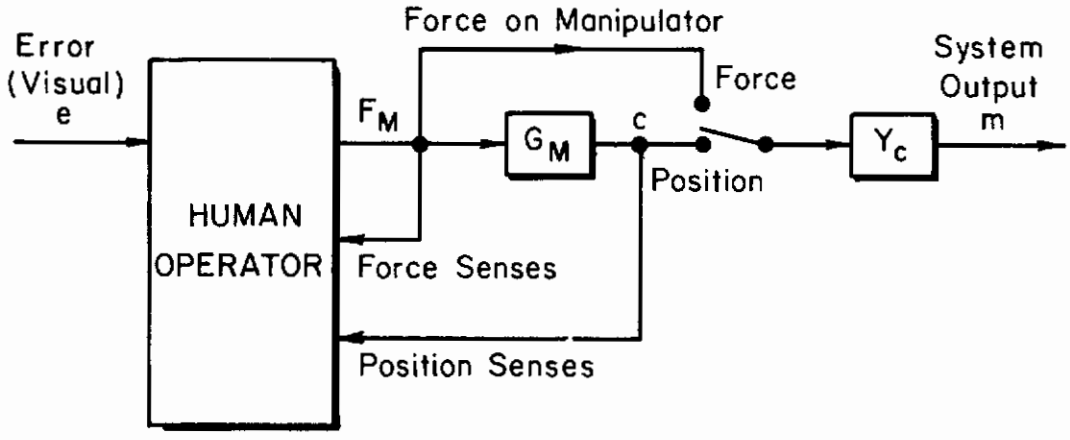

G_M = manipulator load characteristics

Figure 2. Total Open-loop System Experimental Configuration

investigated before, as have spring-restrained manipulators wherein the difference between force and displacement outputs is indistinguishable.

This apparatus configuration was especially contrived to investigate the ability of the human operator to change his force and/or position feedbacks when such a procedure is desirable to obtain good control. This configuration is similar to the one used in Ref. 4.

B. NEUROMUSCULAR SYSTEM FUNCTION DESCRIPTION AND IMPLICATIONS

A view of the neuromuscular system portion of the human operator model which was current at the experimental planning stage is presented in the simplified block diagram representation in Fig. 3. This block diagram is a control system engineering model. As such it is a functional rather than structural analog of the human. The loop structure adopted is intended primarily to be the minimum necessary to exhibit behavior representative of the human operator's neuromuscular system. (Note that in Fig. 2 the load, G_M,

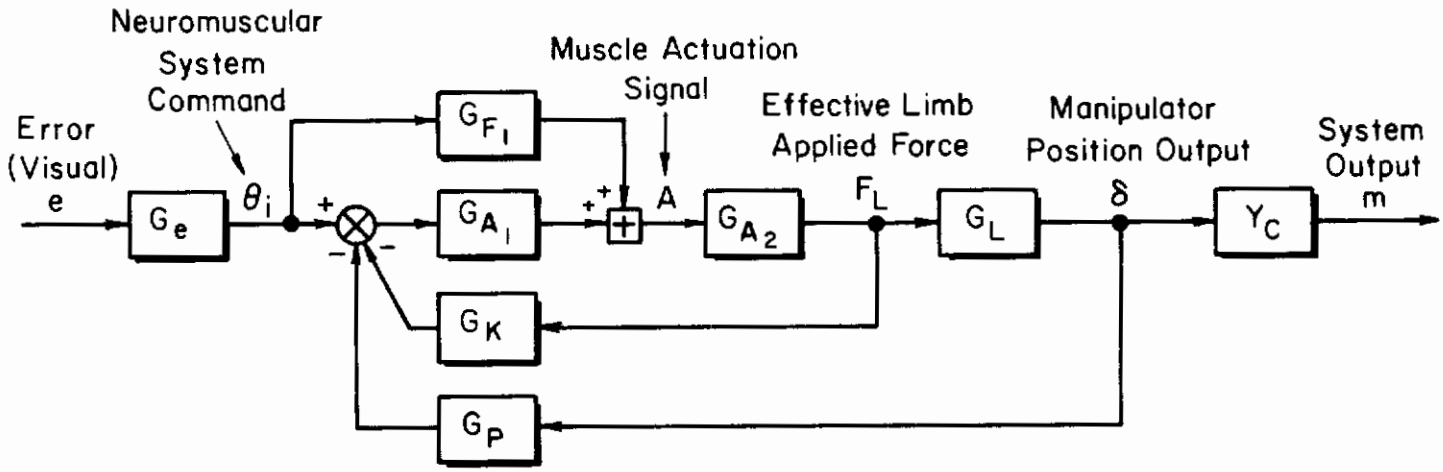

where G_e = input dynamics, central computational delays, equalization and gain adjustment, synaptic and conduction delays to spinal centers involved, etc.

G_{A_1}, G_{A_2} = actuation elements

G_{F_1} = command feedforward

G_K = force feedback elements

G_L = load characteristics of output member and manipulator

G_P = position feedback elements

Y_c = controlled element dynamics

Figure 3. Total Open-Loop System for Position Control

and the human operator are shown as separate entities, while in Fig. 3 the manipulator load characteristics have been absorbed into G_L, involving the dynamics of the manipulator system and the human operator's motor system.) This model was used to help establish the experimental plan.

The block G_e represents the basic equalization capability of the human operator given by the terms $(T_L j\omega + 1)/(T_I j\omega + 1)$ in Eq. 1. Also included in G_e are input dynamics, central computation delays, synaptic and conduction delays to spinal centers involved, etc. The purpose of the command feedforward, G_{F_1}, is to provide a signal path that bypasses some of the neuromuscular system time delays and lags. Such an element is necessary to explain pursuit-like operations and the zero time delay follow-up of recognizable input signals (see, e.g., the Successive Organization of Perception (SOP) theory, Ref. 6). The actuation elements, G_{A_1} and G_{A_2}, contribute lags which tend to show up in the third-order neuromuscular system elements in Eq. 1. As currently conceived, the force feedback element, G_K, consists primarily of Golgi tendon organs which have a moderately high threshold, i.e., they may be inactive unless forces are relatively large. The position feedback element, G_P, represents an ensemble of muscle spindles. An additional input into the box G_P, not shown in Fig. 3, is used to set the gain of the outer loop. The details of this input signal are beyond the scope of this report, although its effect will be briefly discussed in subsequent paragraphs.

The components of the motor-manipulator system element, G_L, are illustrated in Fig. 4. For some manipulators the dynamics may be somewhat more complicated than those shown, although the spring-inertia-damper combination is sufficiently general to describe many situations of practical interest. The external force, F_E, can represent a variety of situations; for example, the output of a force stability augmenter system.

The human elements of the system are actually far more complex than implied by the simple force-mass-damper-spring combination shown. A given motor system is not, in general, a single lumped mass; instead, several coordinates are actually present. For small motions, a single effective lumped mass can be used to represent the lowest frequency characteristics.

The value of this effective mass will depend, of course, on the muscle groups and body memebers being activated. For the pitch control task that was used in this study, the mass of the forearm and upper arm acting on the 4 in. control stick radius yields an effective inertia on the order of three times the minimum stick inertia. This results in essentially a restraintless controller which can be compared with the free-moving control used in the roll axis studies (Ref. 8).

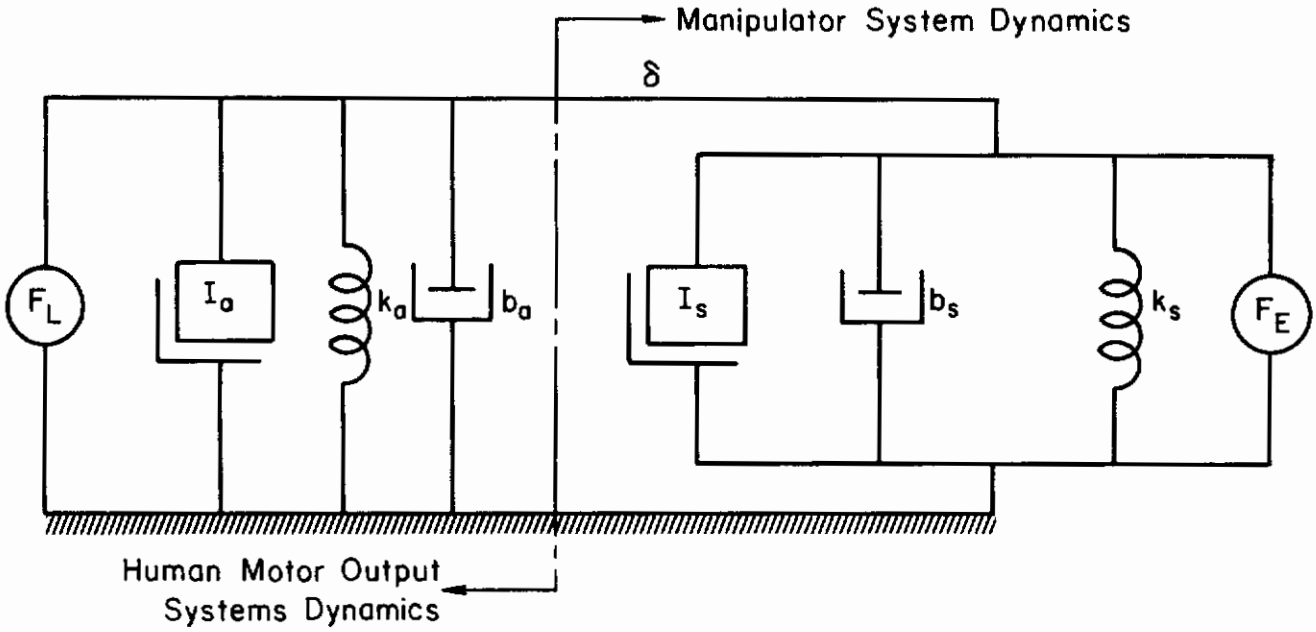

Figure 4. Schematic Diagram of the Motor Load Dynamics

The presence of the spring in the human motor output system follows from a general review of physiological data, which show that the properties of the muscles as affected by the additional input to the position feedback box, G_P, indicate an effective spring rate for muscle behavior. The internal damping element, b_a, is also indicated physiologically. These plus the applied force, F_L, are the major elements contributed by the human.

The equation of motion for the motor-load dynamics is

$$F_L - F_E = \left[(I_a + I_s)s^2 + (b_a + b_s)s + (k_a + k_s)\right]\delta \qquad (4)$$

or when F_E is zero

$$\frac{\delta}{F_L} = G_L = \frac{1}{(I_a + I_s)s^2 + (b_a + b_s)s + (k_a + k_s)} \qquad (5)$$

The closed-loop version of this second-order form is given in the neuromuscular terms of Eq. 1. Increasing the stick inertia or decreasing the stick spring rate decreases the natural frequency of the limb-manipulator system. The effective load dynamics, G_L, could be measured using cross-spectral techniques when F_E is zero and a signal proportional to F_L is available. In this condition,

$$G_L = \frac{\Phi_{i\delta}}{\Phi_{iF_L}} = \frac{1}{(I_a + I_s)s^2 + (b_a + b_s)s + (k_a + k_s)} \qquad (6)$$

from which $I_a + I_s$, $b_a + b_s$, and $k_a + k_s$ can be deduced. The manipulator system dynamic parameters, I_s, b_s, k_s, can be measured separately. Then using these two sets of measurements, one can determine the effective values of I_a, b_a, and k_a which constitute those internal portions of the operator's load characteristics.

From Fig. 3 a signal related to F_L is A, the muscle actuation signal (Electromyograph Signal). These signals have been used to drive artificial arms (e.g., Ref. 7). A limited number of runs were included in the experimental program; but due to difficulties in signal pickup, noise, and interpretation of active muscle groups, the data must be considered preliminary.

1. Position Control

Since signals internal to the human operator cannot be picked off easily, the effects on the overall measurements of the various blocks will be inferred by considering the describing function for the total open-loop system of Fig. 3 given by

$$\frac{m}{e} = \frac{(G_F + G_A)G_eG_LY_c}{1 + G_A(G_K + G_PG_L)} \tag{7}$$

where $G_A = G_{A_1}G_{A_2}$

$G_F = G_{F_1}G_{A_2}$

Except at the very lowest and very highest frequencies of interest in manual control, the neuromuscular system has at least one of its feedback loops fairly tightly closed, i.e., $1 + G_A(G_K + G_PG_L) \doteq G_A(G_K + G_PG_L)$. The open-loop describing function then becomes

$$\frac{m}{e} = \left(1 + \frac{G_F}{G_A}\right)\frac{G_eG_LY_c}{G_K + G_PG_L} \tag{8}$$

G_A is the describing function for the open-loop dynamics of the muscles, while the feedforward element, G_F, was introduced originally into Fig. 3 as a likely means to reduce effective time delays for internally generated commands. Therefore, because of their nature, neither G_F nor G_A should change materially with changes in the form of G_L and Y_c. Consequently, the open-loop describing function in terms of quantities likely to vary with changes in the task variables (Y_c or the manipulator restraints) is given by

$$\frac{m}{e} \propto \frac{G_eG_LY_c}{G_K + G_PG_L} \tag{9}$$

Assuming that the force and displacement feedback quantities, G_K and G_P, can be varied by the pilot as needed to maintain reasonable neuromuscular system dynamics, the relative proportions of each needed to maintain satisfactory neuromuscular system characteristics will vary as G_L is changed. Further, the total range of this variation may be constrained by the nature of the required m/e describing function demanded by the controlled element dynamics, Y_c. From these considerations, it

should be plain that the nature and extent of the variations of G_K and G_P can be investigated readily by making appropriate changes in Y_c and G_L. For instance, systems consisting of pure-inertia manipulator plus pure-gain controlled element, pure-damping manipulator plus an integrator controlled element, or pure-spring manipulator plus a double-integrator controlled element all look like K_c/s^2 if pilot output is force (i.e., if $G_P = 0$), but on a displacement basis ($G_P \rightarrow \infty$) look like K_c, K_c/s, and K_c/s^2, respectively.

As an example of what might occur under limiting case conditions, i.e., $G_PG_L \gg G_K$ or $G_K \gg G_PG_L$, consider the comparative measurements for a pure-inertia manipulator with those for a pure-spring manipulator, both with controlled elements of $Y_c = K_c$ and $Y_c = K_c/s^2$. System "goodness" (performance and stability considerations) requires that m/e be laglike in form, $|m/e| \doteq |\omega_c/j\omega|$, in the region of crossover. The G_e's needed to accomplish this approximate $|\omega_c/j\omega|$ form for these control situations are noted below for the two limiting conditions of the neuromuscular system, tight position loop ($G_PG_L \gg G_K$) and tight force loop ($G_K \gg G_PG_L$), given in Table I. The elements G_P and G_K are assumed to be constants for the mid-band frequencies of interest.

TABLE I

REQUIRED G_e'S FOR POSITION CONTROL

MANIPULATOR AND CONTROLLED ELEMENT DYNAMICS		REQUIRED G_e FOR $\lvert m/e \rvert \doteq \lvert \omega_c/j\omega \rvert$	
		Tight position loop $G_PG_L \gg G_K$ $\left(\frac{m}{e} \propto G_eY_c\right)$	Tight force loop $G_PG_L \ll G_K$ $\left(\frac{m}{e} \propto G_eG_LY_c\right)$
Restraint	Y_c		
Inertia	K_c	Lag	Lead
	K_c/s^2	Lead	Triple lead
Spring	K_c	Lag	Lag
	K_c/s^2	Lead	Lead

To some extent the distinctions noted in the table may be difficult to realize, for one cannot be sure from Y_p measurements alone whether position feedback is dominant or whether the pilot has changed the equalization form in G_e. However, position feedback is most appropriate for the pure-inertia manipulators as a means for reducing the substantial lead equalization requirements otherwise needed in G_e.

Thus, the human operator will most likely attempt to achieve a tight position feedback loop when controlling a pure-inertia manipulator because the G_e equalization requirements are less than those for a tight force feedback loop. Specifically with a tight force feedback, triple lead equalization in G_e is necessary for the K_c/s^2 controlled element. It is highly unlikely that the operator can generate such extreme equalization. For the pure-spring manipulator the required G_e is the same regardless of which feedback loop is tight. Comparison of measurements for the two manipulators should indicate the degree to which the position loop can be "tightened."

2. Force Control

If the stick force transducer output is used as the input to the controlled element, as shown in Fig. 5, the block diagram must be modified by splitting G_L into G_M, relating the force on and position of the manipulator, and G_L/G_M relating the limb applied force, F_L, and the force on the manipulator, F_M (note F_M is the force across the interface in Fig. 4).

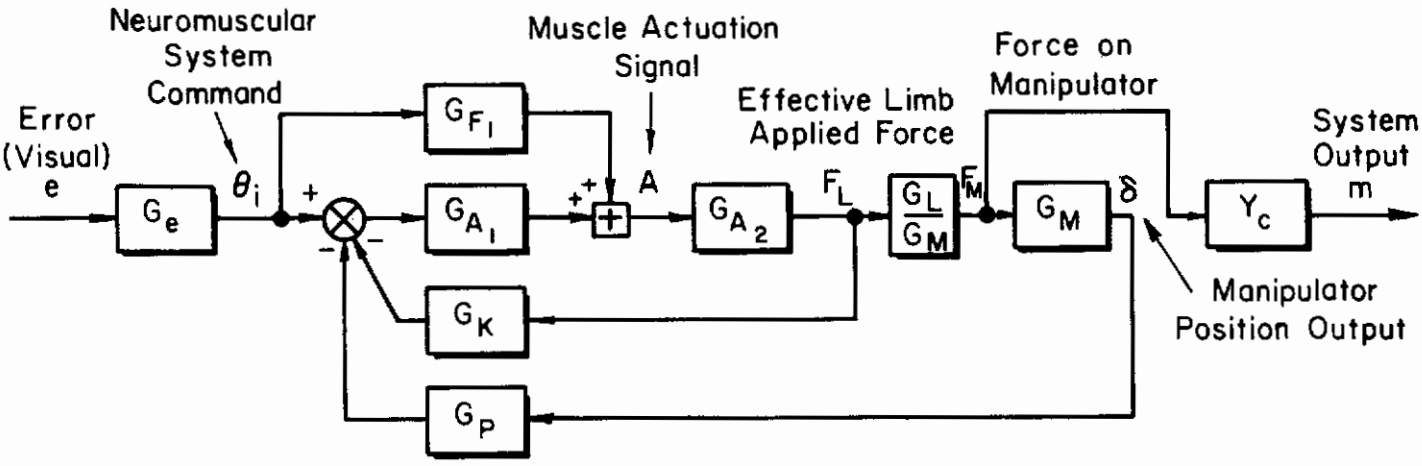

Figure 5. Total Open-Loop System for Force Control

where $$G_M = \frac{1}{I_s s^2 + b_s s + k_s} \tag{10}$$

$$\frac{G_L}{G_M} = \frac{I_s s^2 + b_s s + k_s}{(I_a + I_s)s^2 + (b_a + b_s)s + (k_a + k_s)} \tag{11}$$

The total open-loop describing function for force control then becomes Eq. 7 divided by G_M or

$$\frac{m}{e} = \frac{(G_F + G_A)G_e Y_c G_L}{\left[1 + G_A(G_K + G_P G_L)\right] G_M} \tag{12}$$

Equation 12 differs from Eq. 7 in the absence of G_M, the manipulator dynamics, from the forward loop. G_L remains in and must still be controlled, but the change in location of G_M modifies the nature of the task-imposed constraints on the operator. For the total system to respond properly $|m/e|$ must still approximate $|\omega_c/j\omega|$ in the region of crossover and again assuming either a tight position or tight force loop Eq. 12 becomes

$$\frac{m}{e} \doteq \left(1 + \frac{G_F}{G_A}\right) \frac{G_e Y_c G_L}{(G_K + G_P G_L) G_M} \tag{13}$$

Using the same assumptions and development as for the position control situation, the required G_e's are shown in Table II.

The control situation with the pure-inertia manipulator presents an interesting conflict regarding the selection of a neuromuscular feedback loop. For the $Y_c = K_c$ controlled element, G_e equalization requirements are less (lag versus triple lag) with a tight force loop. In addition, the manipulator position by itself is useless information as far as controlling Y_c, so to the extent that the operator can ignore manipulator position information it is expected that he will attempt to achieve a tight force feedback loop. However, for $Y_c = K_c/s^2$ the required equalization is less demanding (lag versus lead) with a tight position feedback

loop. In fact, this equalization is less difficult to generate than that required for the pure-spring manipulator with the same controlled element, regardless of the feedback loop tightened (lead required in both cases).

TABLE II

REQUIRED G_e'S FOR FORCE CONTROL

MANIPULATOR AND CONTROLLED ELEMENT DYNAMICS		REQUIRED G_e FOR $\lvert m/e \rvert \doteq \lvert \omega_c/j\omega \rvert$	
		Tight position loop $G_P G_L \gg G_K$ $\left(\frac{m}{e} \propto \frac{G_e Y_c}{G_M}\right)$	Tight force loop $G_P G_L \ll G_K$ $\left(\frac{m}{e} \propto \frac{G_e Y_c G_L}{G_M}\right)$
Restraint	Y_c		
Inertia	K_c	Triple lag	Lag
	K_c/s^2	Lag	Lead
Spring	K_c	Lag	Lag
	K_c/s^2	Lead	Lead

C. SUMMARY OF PRE-EXPERIMENT ANALYSIS

The analysis has suggested a couple of critical experiments. For the position control configuration the combination of large inertia plus a double integrator controlled element requires extreme lead equalization capabilities if the pilot doesn't have good position feedback. For the force control configuration with large inertia and a pure-gain controlled element extreme lag equalization will be required unless the pilot can ignore position information (the appropriate thing to do). These two configurations will be included in the experimental plan discussed in Section IV.

SECTION III

EXPERIMENTAL APPARATUS AND FORCING FUNCTION

The measurement situation was as follows. For position control tasks the pilot manipulated a stick (Fig. 6) which produced, as an electrical output signal, the pilot's limb position, c(t), which was fed to the controlled element, Y_c (refer to Figs. 2 and 3). For force control tasks a strain gauge produced an electrical output signal which was fed to the controlled element, Y_c (refer to Figs. 2 and 5). The system error (difference between the input and the controlled element output) was presented on a cathode ray oscilloscope display. Typically, the eye-to-scope distance was about 29 inches.

For position control tasks and $Y_c = K_c$ the circuit gains were set so that $K_c = K_1$ gives the following deflection sensitivity on the display:

$$K_1 = 1 \text{ inch (display)}/6 \text{ deg (stick)}$$

For the 4 inch stick moment arm, longitudinal motion of the operator's hand amounts to about 0.07 inches (stick) per degree of stick rotation. Accordingly, the sensitivity can be expressed in terms of the linear motion of the operator's hand by dividing the angular sensitivity (in inches per radian) by the moment arm, i.e.,

$$K_1 = 1 \text{ inch}/6 \text{ deg} \times 57.3 \text{ deg/rad} \times 0.25 \text{ inch}^{-1} = 2.38 \text{ inches/inch}$$

For position control tasks and $Y_c = K_c/s^2$ setting $K_c = K_a$ gives

$$K_a = 0.2 \text{ inches/sec}^2 \text{ (display) per deg (stick)}$$

For force control tasks and $Y_c = K_c$ setting $K_c = K_{F_1}$ gives a force control sensitivity of $K_{F_1} = 8.77$ inches (display)/ft-lb (stick). For $Y_c = K_c/s^2$ setting $K_c = K_{F_a}$ gives $K_{F_a} = 10.5$ inches/sec^2 per ft-lb (stick). In addition, when the manipulator is clamped (pressure controller) the torque-displacement relationship was found to be 79.8 ft-lb/rad.

The pitch axis of the manipulator shown in Fig. 6 was used for the various manipulator restraints experiments. The roll axis, which didn't have changeable restraint capability, was used in the Ref. 8 experimental series. The pitch axis inertia was variable over a 1500:1 range with the smallest value about one-third of the inertia given by the pilot's limb acting on a 4 inch radius. The largest inertia was considerably larger than any likely to be encountered in flight control systems with bobweight. The range of restraints used was (damping and negligible):

$$\text{Inertia} \quad \begin{cases} I_{min} = .0048 \text{ ft-lb-sec}^2/\text{rad} \\ I_{max} = 7.25 \text{ ft-lb-sec}^2/\text{rad} \end{cases}$$

$$\text{Spring Rate} \quad \begin{cases} k_{min} = 0 \\ k_{max} = 27.2 \text{ ft-lb/rad} \end{cases}$$

Particular values used in Fig. 7 (next chapter) are:

$$k_1 = 1.09 \text{ ft-lb/rad}$$
$$I_1 = 0.29 \text{ ft-lb-sec}^2/\text{rad}$$

A four minute run length was used. As in Ref. 1, the forcing function used was a sum of six equal amplitude sine waves with a bandwidth of 2.5 rad/sec, augmented by four high frequency sine waves each 20 db less than any of the low frequency group. The highest of the augmenting frequencies is 14 rad/sec. In the notation of Ref. 2 this is a B6 input. In the next section the present pitch axis data will be compared with the roll axis data taken with a B5 input (Ref. 8). The B5 input is the same as the B6 except that the augmenting frequencies are only 10 db less than any of the low frequency group. Note that these inputs have different effective bandwidths which may compromise the pitch axis-roll axis comparison. The above comparison is aided by the inclusion of data taken with an R0.40 input. This is unpublished data from a preliminary set of experiments in a series that is reported in Ref. 8.

The R0.40 is a sum of six equal amplitude sine waves with a bandwidth of 0.40 cps or 2.5 rad/sec. Thus the B6 inputs effective bandwidth is intermediate to that for the R0.40 and B5 inputs.

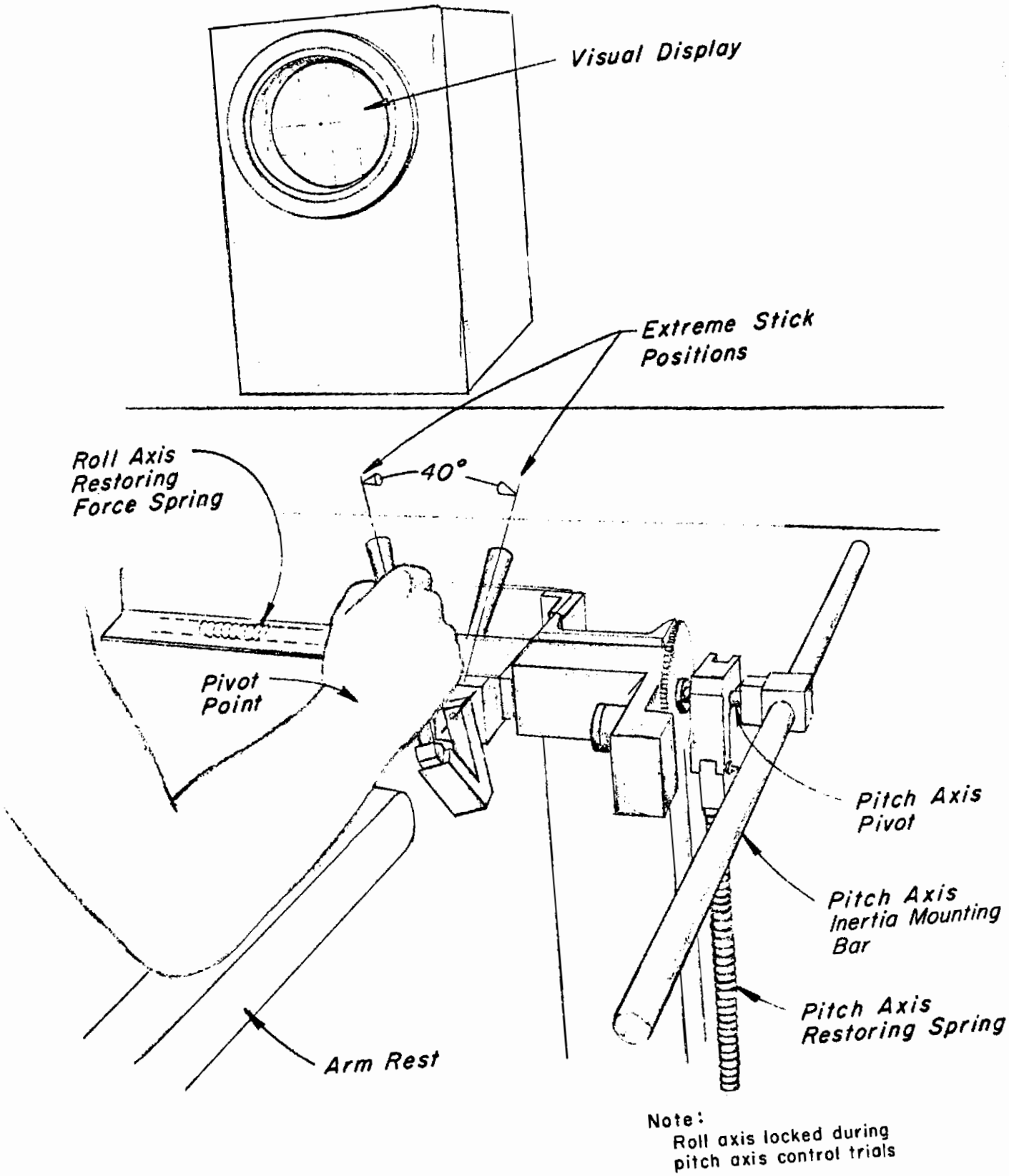

Figure 6. Stick Manipulator

SECTION IV

EXPERIMENTAL DESCRIBING FUNCTION DATA AND INTERPRETATIONS

A. EXPERIMENTAL PLAN

This chapter presents the experimental matrix and the describing function data obtained for the investigation. The data will be presented in various aggregations designed to illustrate and illuminate the findings. Each set of data taken was an element in a grand design conceived to fulfill the experimental objectives discussed in Section II plus some to be discussed in this section. The resulting experimental matrix is shown in Figs. 7 and 8.

Not shown in Fig. 7 is an indication of the subjects and forcing functions used. These were restricted to one of each to keep the program down to a reasonable size. In addition not all the spring rate, inertia, and controlled element combinations shown in Fig. 7 were tested, since at the minimum of three runs per configuration actually used this would have resulted in a very large number of runs. Instead, the matrix, as indicated in Fig. 8, has selectively filled in those particular blocks where the findings would shed the most light on load effects. The circled numbers in the boxes indicate configurations used in the describing function comparisons. As discussed in Section III, the forcing function task variable was the augmented rectangular spectrum with bandwidth ω_i = 2.5 rad/sec, with σ_i = 1/2" for $Y_c = K_c$, and σ_i = 1/4" for $Y_c = K_c/s^2$. For $Y_c = K_c$, exceptions were for the force control inertia variable and for configurations 4, 5, 6, and 7 where σ_i = 1/4". The subject was a light-airplane-qualified civilian pilot with extensive tracking experience who had participated in all the STI-FIL experiments discussed in Ref. 1, and who was the sole subject in the various manipulators experiments (Ref. 8). Because of this extensive experience the subject was able to rapidly approach asymptotic values of performance on any given configuration, thereby permitting a large number of configurations to be examined at minimal cost. While more subjects would have been desirable, the exploratory and limited-effort nature of the experimental series made this unrealistic. To make the results as representative as possible, considerable efforts were made to tie-in to other data, including situations wherein the subject had already been shown to be reasonably representative of pilots in tracking situations (Ref. 1).

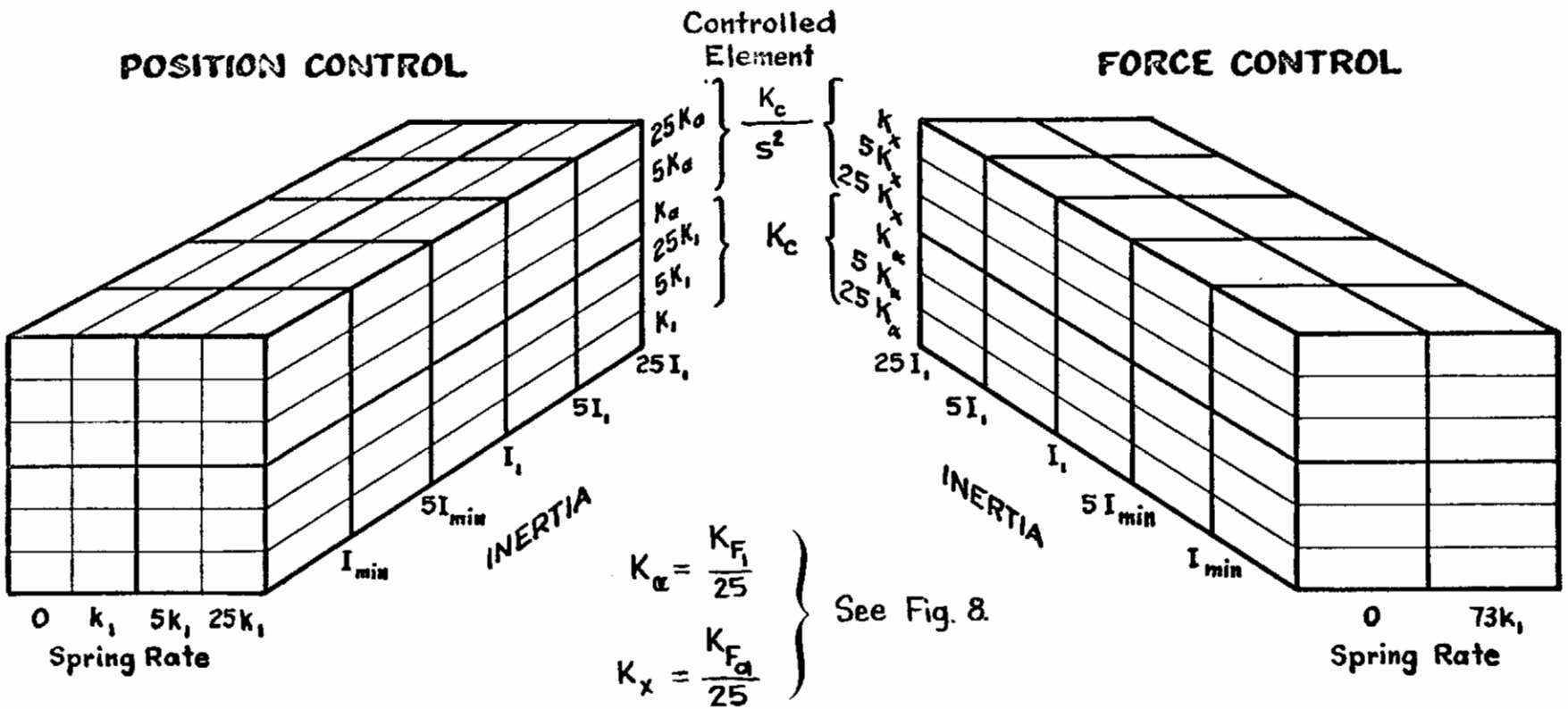

Figure 7. Various Manipulator Restraints Matrix

CONTROLLED ELEMENT Y_c	POSITION CONTROL TASKS										FORCE CONTROL TASKS			
	Position Control Sensitivity	Inertia Restraint (no spring) I_m = minimum inertia						Spring Restraint (minimum inertia) $I = I_m$			Force Control Sensitivity	Pressure Controller (stick clamped)	Inertia Restraint (no spring)	
		I_m	$5I_m$	$25I_m$	I_1	$5I_1$	$25I_1$	k_1	$5k_1$	$25k_1$			$25I_1$	$5I_1$
K_c	K_1	①	②		③	④	⑤	⑧	⑨	⑩	K_{F_1}	㉓	㉖	㉗
	$5K_1$					⑥			⑪		$K_{F_1}/5$	㉝		
	$25K_1$						⑦			⑫	$K_{F_1}/25$	㉞		
K_c/s^2	K_a	⑬	⑭	⑮	㉚	㉛	㉜	⑱	⑲	⑳	K_{F_a}	㉔	㉘	㉙
	$5K_a$		⑯						㉑		$K_{F_a}/5$	㉕		
	$25K_a$			⑰						㉒	$K_{F_a}/25$	㉟		
$K_1 = \frac{1 \text{ in.(display)}}{6 \text{ deg (stick)}}$ or $K_1 = \frac{9.55 \text{ in.(display)}}{\text{rad (stick)}}$ $K_a = 1.2K_1$		$I_m = 0.0048 \frac{\text{ft-lb-sec}^2}{\text{rad}}$ $I_1 = 0.29 \frac{\text{ft-lb-sec}^2}{\text{rad}}$ $25I_1 = 7.25 \frac{\text{ft-lb-sec}^2}{\text{rad}}$ $25I_1 = 1500 I_m$						$k_1 = \frac{1.09 \text{ ft-lb}}{\text{rad}}$ $k_1 = \frac{0.82 \text{ lb}}{\text{in.}}$ at top of 4 in. stick $\sqrt{\frac{k_1}{I_m}} = 15 \text{ rad/sec}$			$K_{F_1} = \frac{K_1}{k_1} = \frac{8.77 \text{ in.}}{\text{ft-lb}}$ $K_{F_a} = 1.2K_{F_1} = \frac{10.5 \text{ in.}}{\text{ft-lb}}$	For Pressure Controller the clamped sticks effective spring rate is $k_c = \frac{79.8 \text{ ft-lb}}{\text{rad}} = 73k_1$ Note that $K_{F_1} = \frac{K_1}{k_1} = \frac{73K_1}{73k_1}$ Thus Conf. ㉓ has a position control sensitivity given by $73K_1$.		

Forcing function bandwidth, ω_i = 2.5 rad/sec. The σ_i's are discussed on p. 21.

Note that the Pressure Controller configurations can also be considered as position control tasks. The effective position control sensitivity can be computed by multiplying the force control sensitivity by the spring rate ($k_c = 73k_1$).

Figure 8. Various Manipulator Restraints Experiments

The configurations indicated in Fig. 8 were selected to fulfill the following experimental objectives:

1. Provide a comparison (tie-in) with either the pressure or free-moving manipulators in Ref. 8 which involved lateral control. For the position control experiments, this is the upper left hand entry in each submatrix. For the current pressure control experiments, the configuration with the best results was used. In addition, a comparison with the matrix of pilots (Ref. 1) results is given by (18) and (21).

2. Investigate the effects of restraint increases from the tie-in configurations (item 1 above).

   a. Spring increase from zero to maximum
   This is given by (1) (8) (9) (10) for $Y_c = K_c$
   and (13) (18) (19) (20) for $Y_c = K_c/s^2$

   b. Inertia increase from I_{min} to I_{max}
   This is given by (1) through (5) for $Y_c = K_c$ and
   (13) (14) (15) (30) (31) (32) for $Y_c = K_c/s^2$

3. Investigate the transition from a free-moving control to a pressure control by increasing the spring rate and the controlled element gain in the same ratio. This reduces the stick position sensitivity while the force sensitivity is constant. Configurations (8) (11) (12) (23) for $Y_c = K_c$ and (18) (21) (22) (24) for $Y_c = K_c/s^2$ provide the comparison.

4. Investigate the effects of the interchange of mechanical restraints with controlled element dynamics (discussed in Sections I.B and II). This is given by comparing (1) and (5) with (18). The first two have $Y_c = K_c$ and inertias of I_{min} and I_{max} respectively while (18) has $Y_c = K_c/s^2$, I_{min} and a spring restraint.

5. Investigate the approach to a pressure controller via large inertia, i.e., the pilot controlling the force on a large inertia should perform as well as with the pressure controller ((23) and (26) for $Y_c = K_c$ and (28) (24) for $Y_c = K_c/s^2$). In addition, the effects of reducing inertia are given by configurations (27) and (29).

B. EXPERIMENTAL DATA

The data will be discussed relative to the objectives outlined above and the summary of the pre-experiment analysis. Frequent reference will be made to the extended crossover model form given by Eq. 3 repeated here.

$$Y_p Y_c \triangleq \frac{\omega_c e^{-j\left(\tau_e \omega + \frac{\alpha}{\omega}\right)}}{j\omega} \qquad (14)$$

where ω_c = crossover frequency

$\tau_e = \tau + T_N - T_{L_{hi}}$

α = approximation to low frequency terms (Eq. 1)

The T_N component of τ_e contains the first-order effects of the neuromuscular system within the measurement bandwidth, i.e.,

$$T_N = \underbrace{T_{N_1}}_{\text{actuation lag}} + \underbrace{\frac{2\zeta_N}{\omega_N}}_{\substack{\text{effective time constant of second-order terms of} \\ \text{motor load dynamics (Eq. 1)}}} \qquad (15)$$

Thus, τ_e will tend to be increased by increases in inertia and decreases in spring rate.

1. Tie-Ins

a. With Pressure and Free-Moving Controllers (Roll Control)

The comparison of the spring-restrained control stick with the pressure and free-moving controllers is shown in Figs. 9 and 10 for $Y_c = K_c$ and Figs. 11 and 12 for $Y_c = K_c/s^2$. In general, the present describing functions and mean square errors fall between the earlier results with the R0.40 and B5 inputs. This is consistent with the present B6 input bandwidth being intermediate to the other two (p. 19). The only exception is for Fig. 11 where the earlier pressure control had a higher crossover frequency in spite of the higher input bandwidth. This implies that pitch axis pressure control is not quite as good as roll control.

b. With matrix of pilots (Fig. 13)

The data from Ref. 1 (spring-restrained sidestick) for $Y_c = K_c/s^2$ is compared with the tie-in configuration (18) and with (21) in Fig. 13. There are slight differences from the matrix of pilots results. The crossover frequency for the matrix of pilots (3.25 rad/sec) was intermediate to that for (18) (2.8 rad/sec) and (21) (3.6 rad/sec). The best of the present configurations, (21), had the same τ_e as the pilots, but apparently a larger α. The difference in mean square

error is partly due to the lower input frequencies used for the matrix of pilots even though the basic envelope was the same. This comparison indicates little difference between pitch and roll tracking for spring-restrained manipulators.

2. Load Effects of Various Restraints

a. Relative RMS error σ_e/σ_i (db), for various Spring Rate and Control Sensitivities

1) $Y_c = K_c$ (Fig. 14)

Relative RMS error is essentially constant for spring rates from zero to maximum (1) (8) (9) (10). Performance decreases if control sensitivity is increased in proportion to spring rate except when spring rate reaches the pressure controller configuration, (8) (11) (12) (23). There is further improvement at the smaller control sensitivities for the manipulator clamped configurations.

2) $Y_c = \frac{K_c}{s^2}$ (Fig. 15)

Relative RMS error has a shallow minimum at an intermediate spring rate and control sensitivity which is significantly better than for zero spring (13). For the pressure controller performance has a minimum at an intermediate control sensitivity. The addition of the spring, at constant control sensitivity, improves performance over that for zero spring, (13) (18) (19), except for the largest spring, 20.

b. Effects of spring increases on pilot describing function

1) $Y_c = K_c$ (Fig. 16)

Although spring increases had no effect on relative RMS error, the crossover frequency is largest for configuration (8), $\omega_c = 6$ rad/sec, dropping off to about 5 rad/sec for no spring (1) and max spring (10). Configuration (8) also has larger low frequency gain although there is no significant change in phase for a large range of spring rates. Also included in Fig. 16 is the best pressure controller configuration, (33). It has the lowest DC gain but one of the highest crossover frequencies (6 rad/sec).

The nearly constant crossover frequency and phase lag can possibly be explained by presuming little change in the position loop gain (since required excursions are unchanged) and some change in force loop gains (since the required forces increase) while

K_p remains more or less fixed. The essentially unchanged amplitude and phase characteristics indicate a fairly tight position loop.

2) $Y_c = \frac{K_c}{s^2}$ (Fig. 17)

Crossover frequency is constant except for a slight decrease for the stiffest spring (20) while τ_e decreases slightly as spring rate increases. The τ_e decreases indicate that the spring increases help push the second order neuromuscular lag to higher frequencies. In addition, the best of the pressure controller configurations, (25), had lower gain at low frequency. This is offset by a lower τ_e in the crossover region such that σ_e/σ_i is about the same as (19).

The basic trend in the data is that k ↑ causes τ_e ↓ which correlates with the findings of the various manipulators experiments (Ref. 8). This trend is modified somewhat by the discussion in Section 3.b. on p. 28.

c. Inertia increases

1) $Y_c = K_c$ (Fig. 18)

Inertia increases cause steady decline in gain and crossover frequency with a proportional increase in σ_e/σ_i. There is little effect on the phase for (1), (2) and (3). These data appear as typical $Y_c = K_c$ data, so the neuromuscular system position loop must be a major factor in retaining the similar forms in the face of such drastic inertia changes. The decrease in gain may be due to actuation limiting since the required forces are increasing roughly proportional to inertia.

The basic effect is

$$I \uparrow \text{ causes } \omega_c \downarrow, \frac{\sigma_e}{\sigma_i} \uparrow, \tau_e \text{ and } \alpha \text{ no change}$$

2) $Y_c = \frac{K_c}{s^2}$ (Fig. 19)

Inertia increases cause steady decline in gain, increase in σ_e/σ_i and an increase in τ_e. There is a resonance at high frequency for the larger inertias. Clearly the inertia increases are reducing ω_N of the second-order neuromuscular lag which affects τ_e and for the larger inertias the break point is within the measurement bandwidth. Here, without question, the position loop of the neuromuscular system plays a central role in retaining the characteristic Y_pY_c

features since the lead equalization capabilities are used up at low frequencies to compensate for the controlled element.

The basic effects to note are (neglecting the highly variable phase data at the lowest frequency)

$$I \uparrow \text{ causes } \omega_c \downarrow, \frac{\sigma_e}{\sigma_i} \uparrow, \tau_e \uparrow, \alpha \uparrow$$

3. Approach toward a pressure controller via increases in position control sensitivity and spring rate such that ratio is constant.

a. $Y_c = K_c$ (Fig. 20)

There is a significant increase in σ_e/σ_i and decrease in ω_c at the larger gains and spring rates improving somewhat for the pressure controller (which has the same force control sensitivity as the spring restraint). The phase changes are small implying a fairly tight position loop. The amplitude changes are not likely to be due to equalization changes since the phase doesn't vary.

b. $Y_c = \frac{K_c}{s^2}$ (Fig. 21)

Intermediate values of spring rate and control sensitivity result in a small increase in ω_c, less σ_e/σ_i, some increase in low frequency gain and a small decrease in τ_e. These observations plus those on the σ_e/σ_i results (Fig. 15) indicate that the intermediate values of spring rate and control sensitivity yield the best performance (Configurations (19), (21), (22), and (25)). The larger spring rates help in increasing the natural frequency of the control stick, thereby helping reduce τ_e while the larger control sensitivities enable smaller stick motions.

4. Pilot as a position versus a force output device — interchange of mechanical restraints with controlled element dynamics.

a. Figure 22 compares the effects of moving a double integration from the manipulator restraint to the controlled element.

Configurations (1) (inertia restraint and $Y_c = K_c$) and (18) (spring restraint and $Y_c = K_c/s^2$) show grossly different pilot behavior. Configuration (1) is typical

of that for $Y_c = K_c$ (Figs. 9 and 16 and Ref. 1) whereas configuration (18) is typical of that for $Y_c = K_c/s^2$. For $Y_c = K_c$ increasing the inertia to its maximum, configuration (5), degrades the amplitude such that it has the same gain and crossover frequency as configuration (18), but the phase is fundamentally different, i.e., the large lagging phase angles at low frequency do not appear. In addition, the σ_e/σ_i is considerably smaller for configuration (5) than for configuration (18). Configuration (13) is also shown in Fig. 22.

These data are strong evidence that the pilot has good position feedback. The basic clues are that:

1) configuration (13) (inertia and $Y_c = K_c/s^2$) is controllable which would require triple lead equalization if the pilot didn't have good position feedback capability (Table I, p. 14)

2) a fundamental difference exists in phase characteristics and performance for essentially the same amplitude characteristics near crossover and above ((5) and (18)).

5. Approach toward a pressure controller via large inertia

a. $Y_c = K_c$ (Fig. 23)

This shows that the pilot, controlling the force on an unrestrained very large inertia performs almost as well as for the pressure controller configuration with the same force sensitivity. Also shown is the effect of reducing the inertia by a factor of 5, for which the pilot reduces his low frequency gain in an attempt to prevent large motions of the inertia. Performance deteriorates slightly and ω_c increases slightly. Smaller values of inertia were tested, as indicated by Fig. 7, but performance rapidly deteriorated as the operator's output motions drove the manipulator against the mechanical stops. The data, particularly configuration (27), show that to a certain extent the pilot can ignore position information when he has to.

b. $Y_c = K_c/s^2$ (Fig. 24)

The comments for $Y_c = K_c$ generally apply here except that inertia reduction causes a reduction in gain both at low and mid-band frequencies.

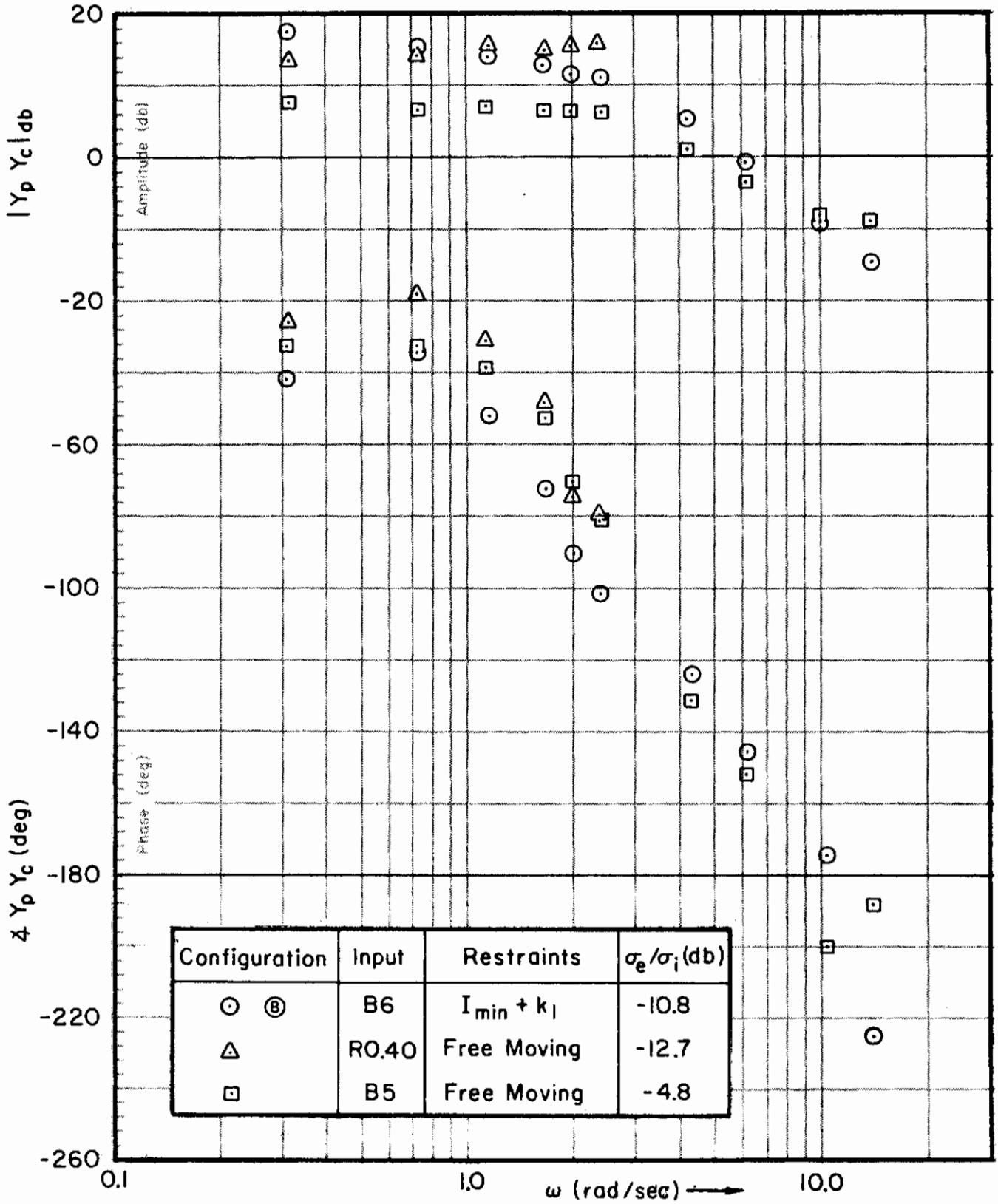

Figure 9. Comparison of Pitch Axis (Spring Restraint) and Roll Axis (Free Moving) Averaged Open-Loop Describing Functions ($Y_c = K_c$)

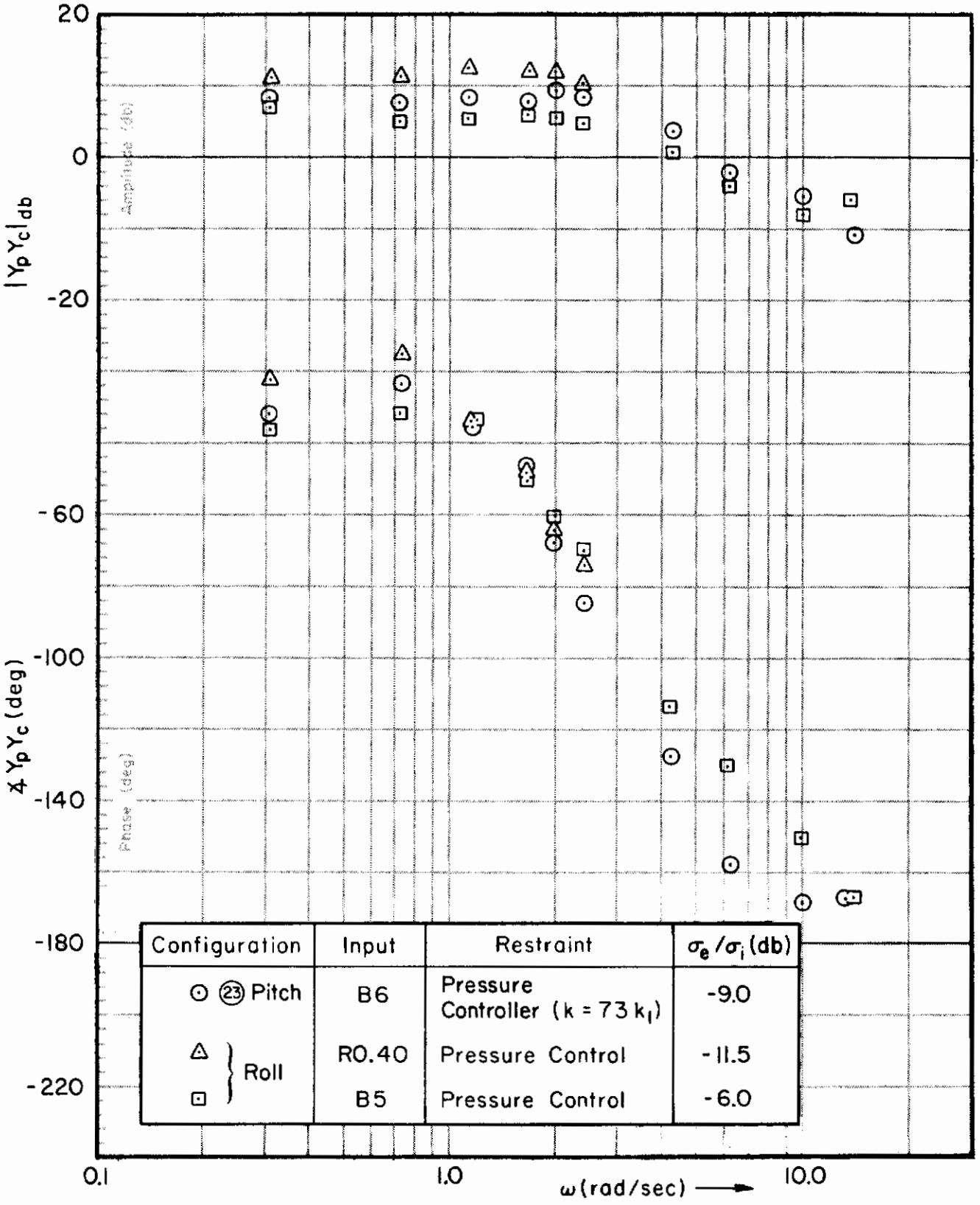

Figure 10. Comparison of Pitch Axis (Pressure Control) and Roll Axis (Pressure Control) Averaged Open-Loop Describing Functions ($Y_c = K_c$)

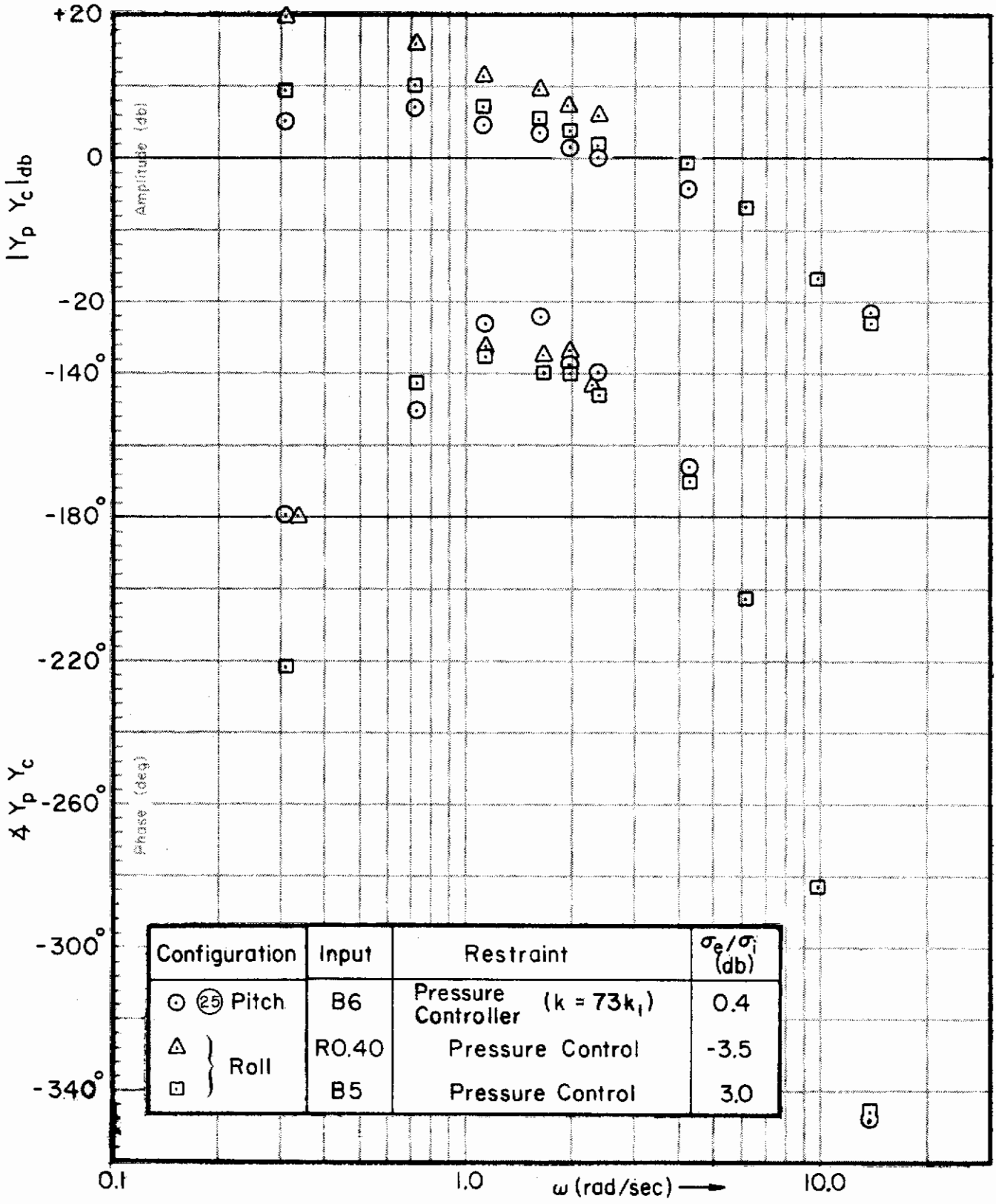

Figure 11. Comparison of Pitch Axis (Pressure Control) and Roll Axis (Pressure Control) Averaged Open-Loop Describing Functions $\left[Y_c = K_c/s^2\right]$

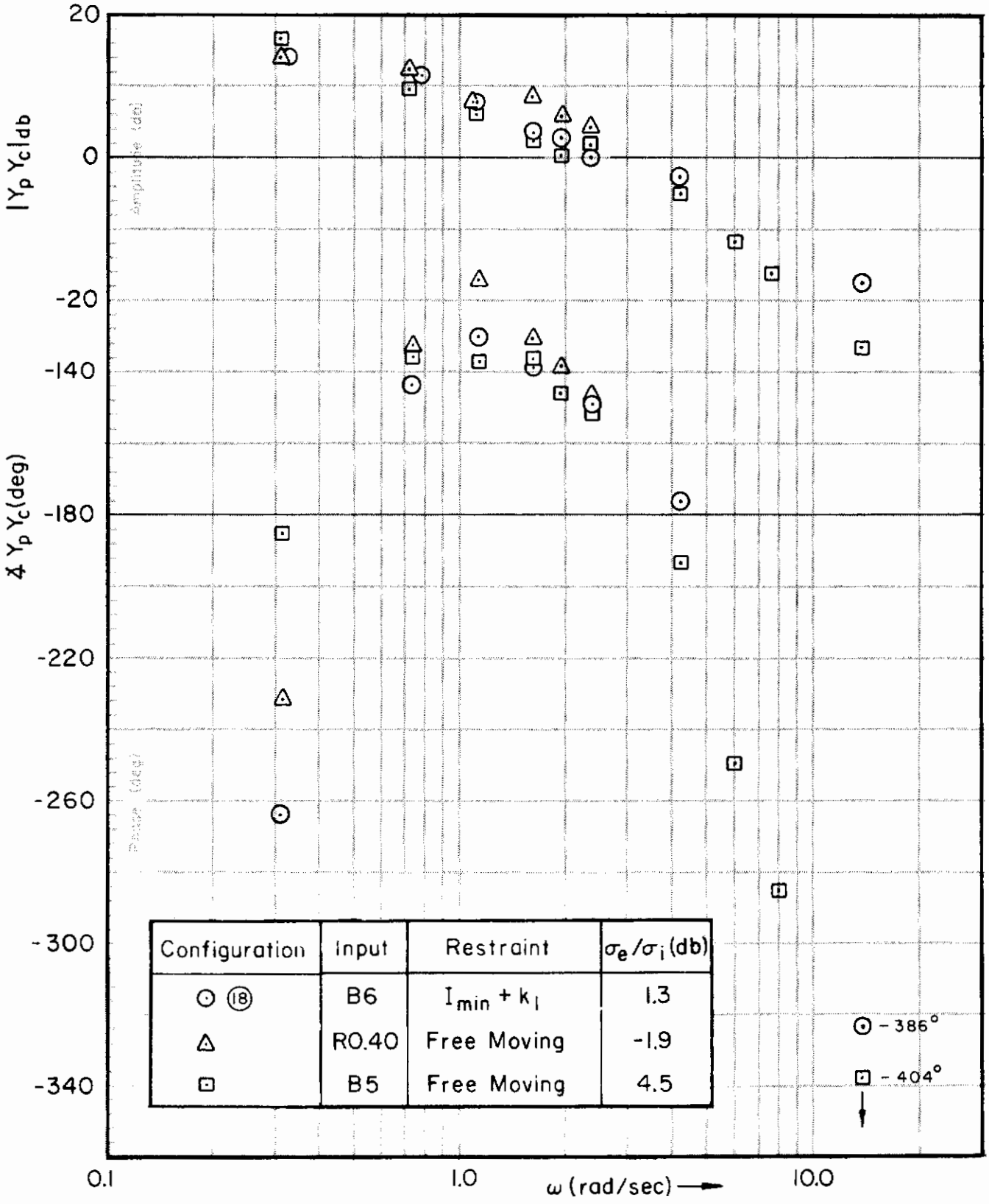

Figure 12. Comparison of Pitch Axis (Spring Restraint) and Roll Axis (Free Moving) Averaged Open-Loop Describing Functions $\left[Y_c = K_c/s^2\right]$

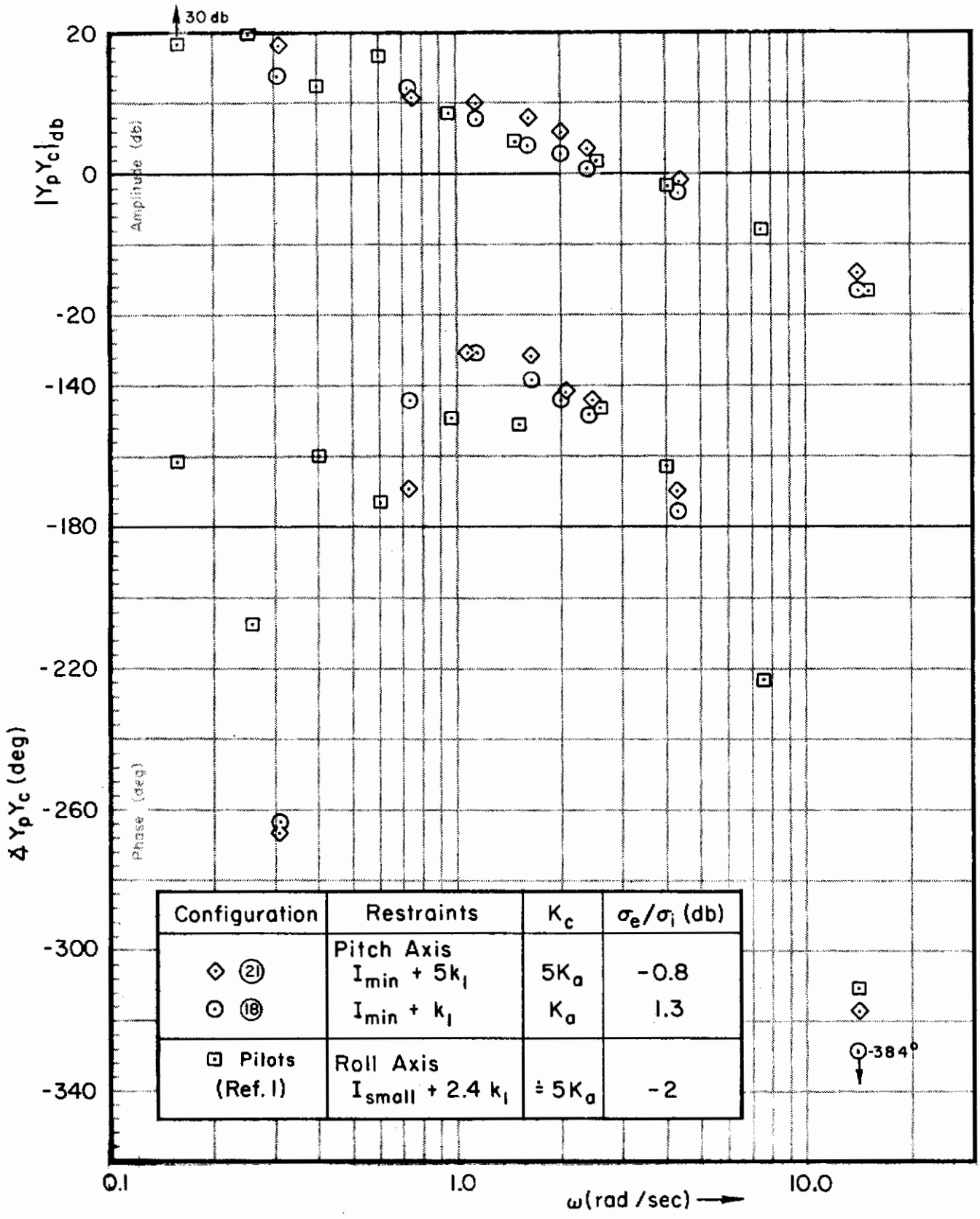

Figure 13. Comparison of Pitch Axis (Spring Restraint) and Roll Axis (Spring Restraint) Averaged Open-Loop Describing Functions $\left[Y_c = K_c/s^2\right]$

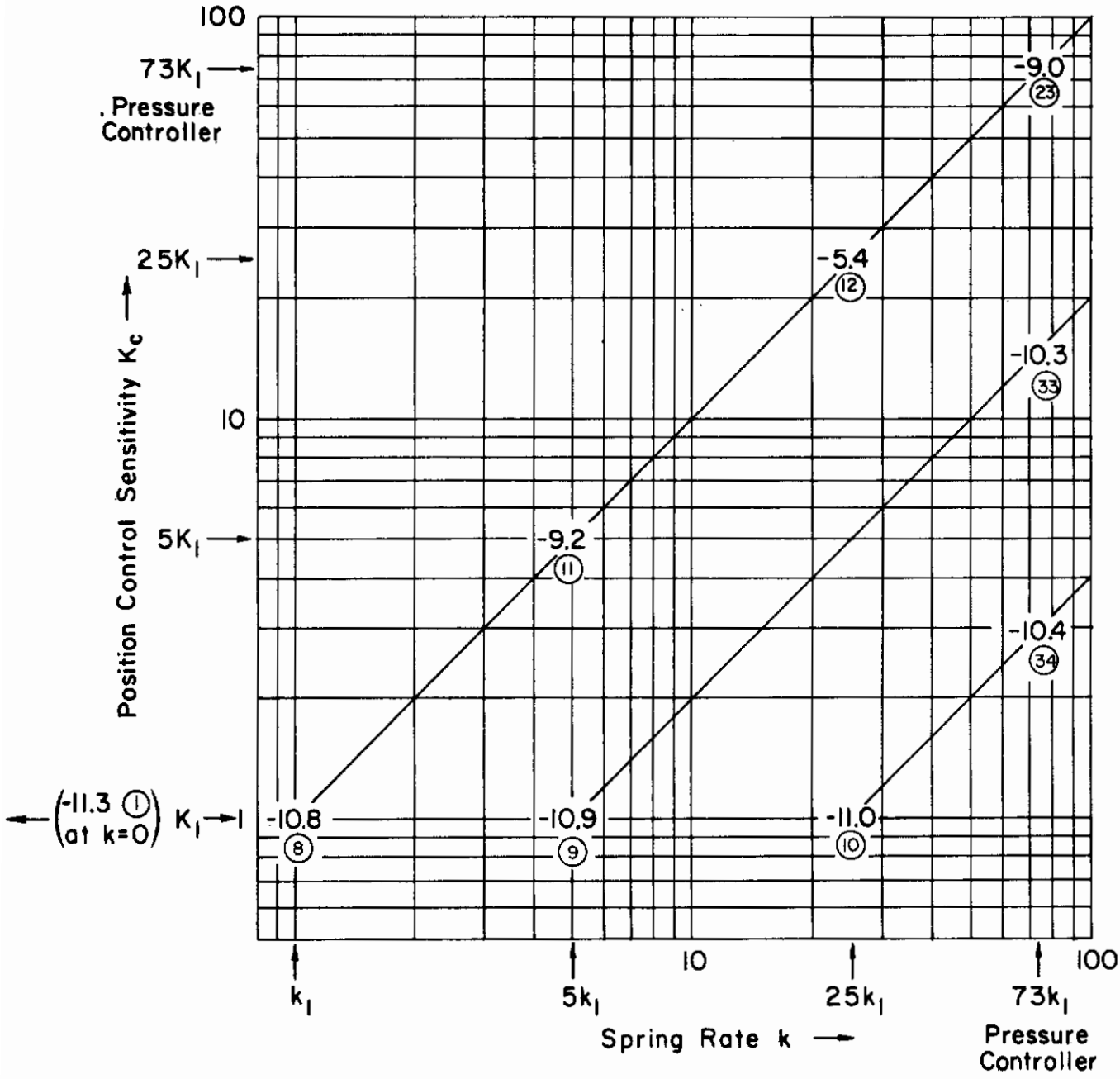

Figure 14. Averaged Relative RMS Error, σ_e/σ_i (db), for Various Spring Rates and Position Control Sensitivities Given by Circled Configuration Number ($Y_c = K_c$)

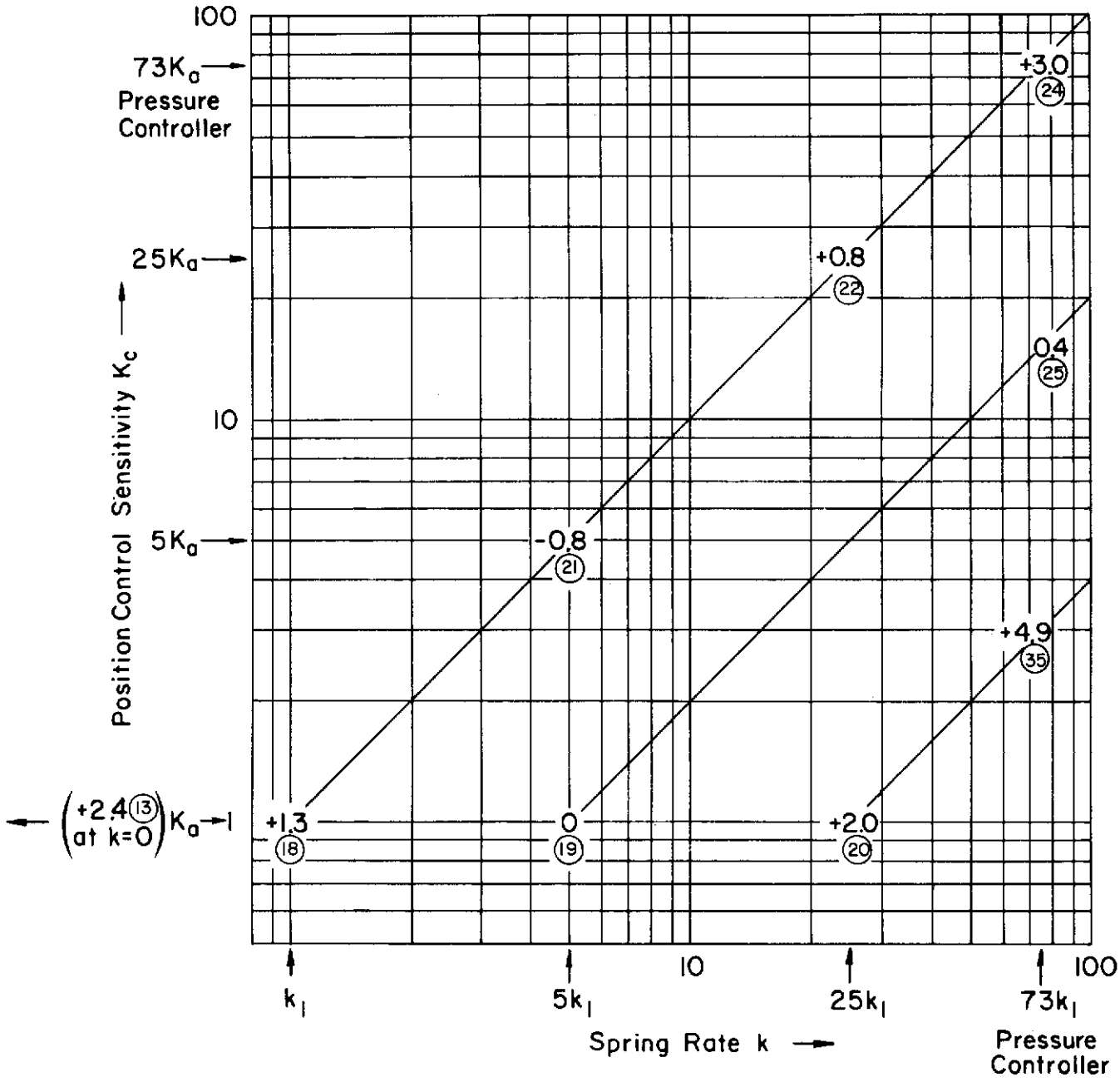

Figure 15. Averaged Relative RMS Error, σ_e/σ_i (db), for Various Spring Rates and Position Control Sensitivities Given by Circled Configuration Number ($Y_c = K_c/s^2$)

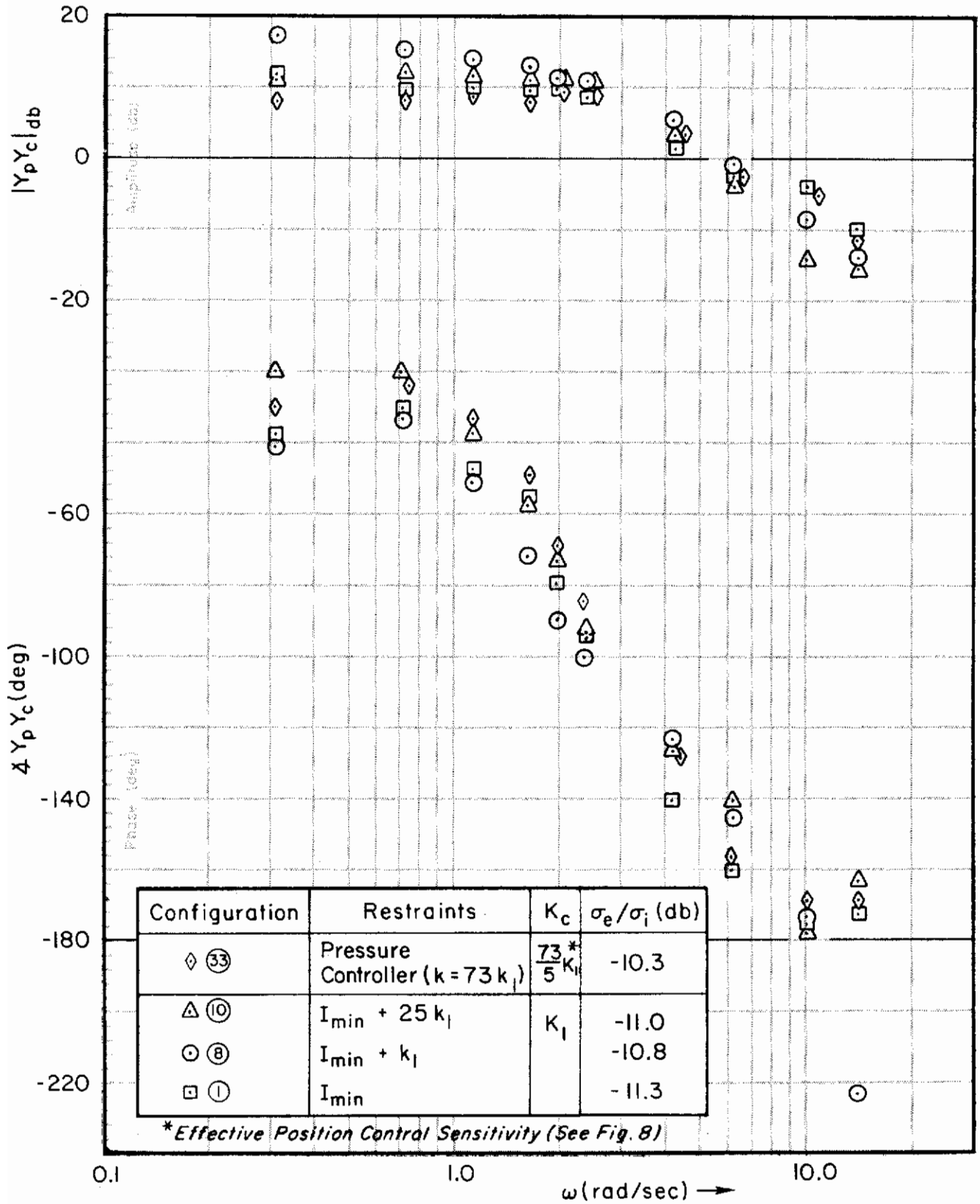

Figure 16. Averaged Open-Loop Describing Functions for $Y_c = K_c$ with Spring Rate as Parameter

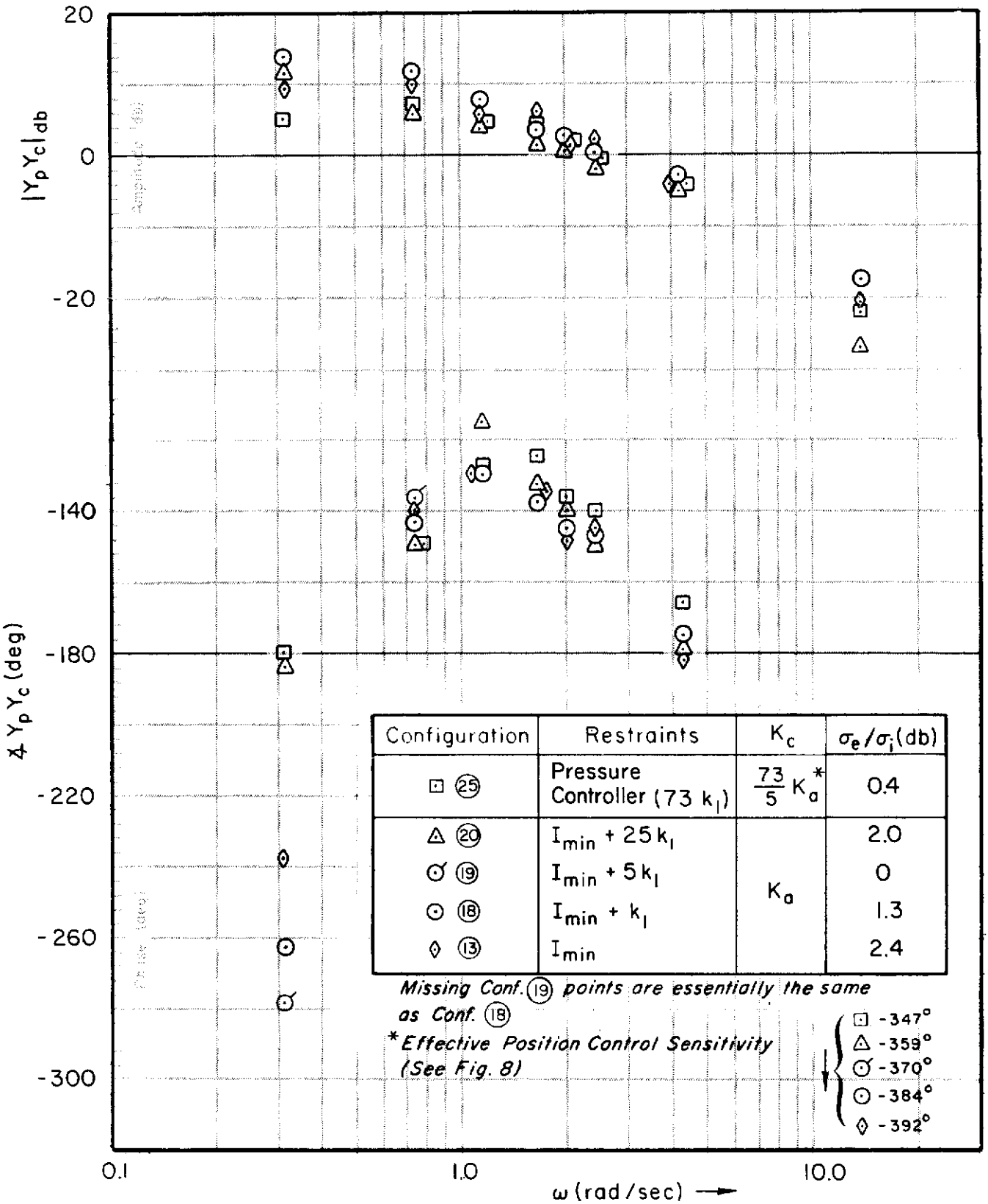

Figure 17. Averaged Open-Loop Describing Functions for $Y_c = K_c/s^2$ with Spring Rate as Parameter

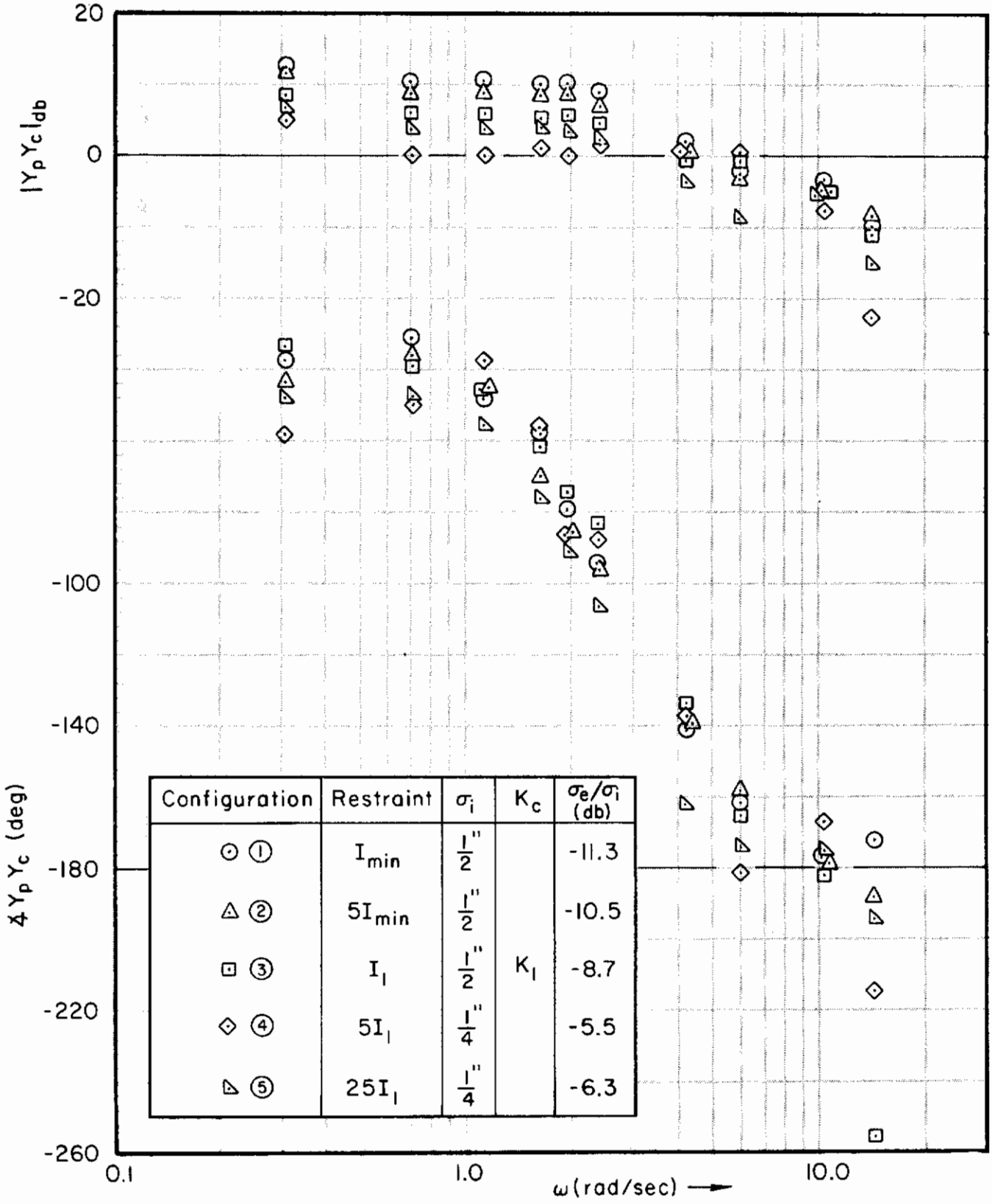

Configuration	Restraint	σ_i	K_c	σ_e/σ_i (db)
⊙ ①	I_{min}	$\frac{1}{2}$"		-11.3
△ ②	$5I_{min}$	$\frac{1}{2}$"		-10.5
⊡ ③	I_1	$\frac{1}{2}$"	K_1	-8.7
◇ ④	$5I_1$	$\frac{1}{4}$"		-5.5
◺ ⑤	$25I_1$	$\frac{1}{4}$"		-6.3

Figure 18. Averaged Describing Functions for $Y_c = K_c$ with Inertia as a Parameter

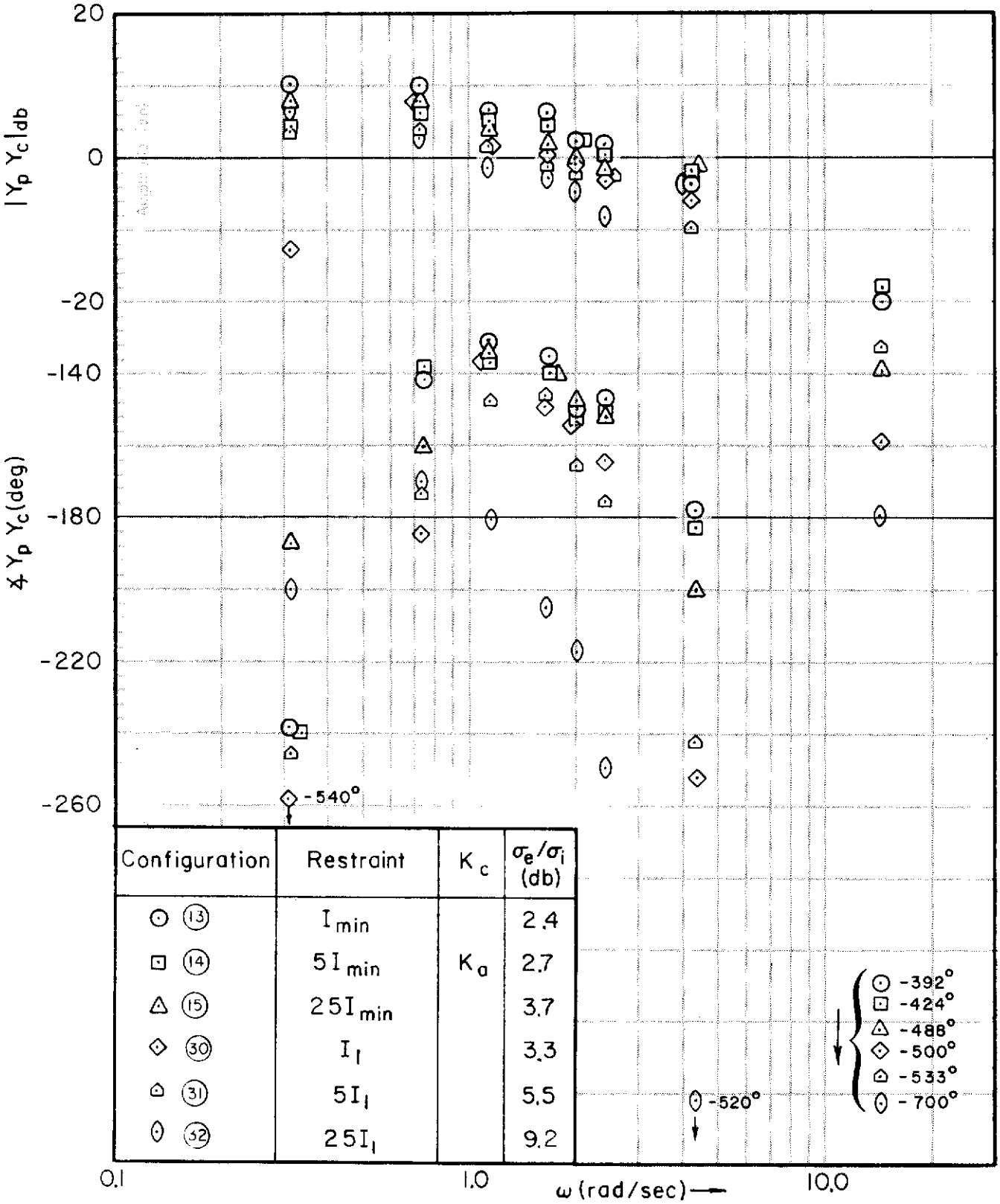

Configuration	Restraint	K_c	σ_e/σ_i (db)
⊙ (13)	I_{min}		2.4
⊡ (14)	$5I_{min}$	K_a	2.7
△ (15)	$25I_{min}$		3.7
◇ (30)	I_I		3.3
⌂ (31)	$5I_I$		5.5
⊙ (32)	$25I_I$		9.2

Figure 19. Averaged Open-Loop Describing Functions for $Y_c = K_c/s^2$ with Inertia as Parameter

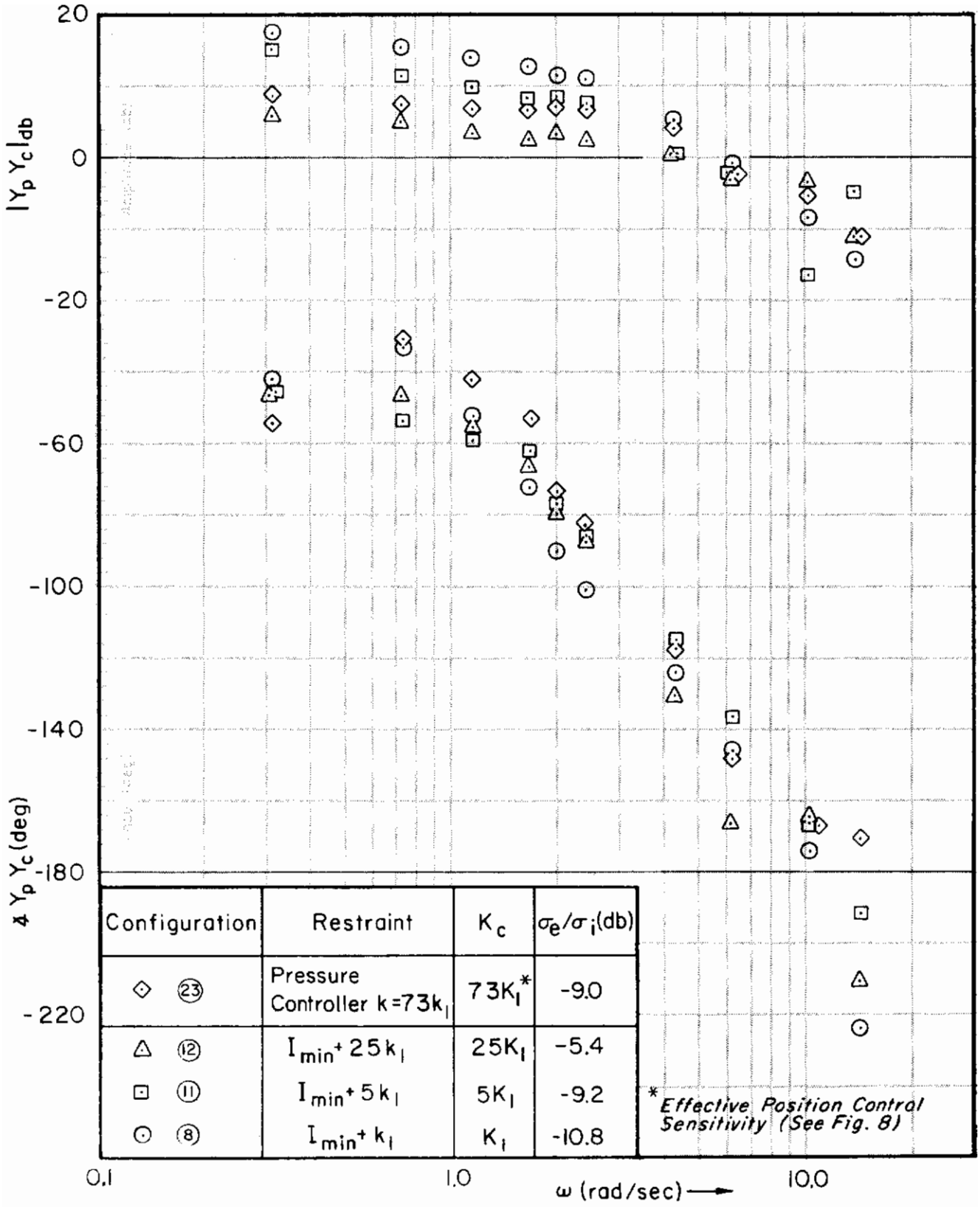

Figure 20. Averaged Open-Loop Describing Functions for Increases in Spring Rate and Control Sensitivity ($Y_c = K_c$)

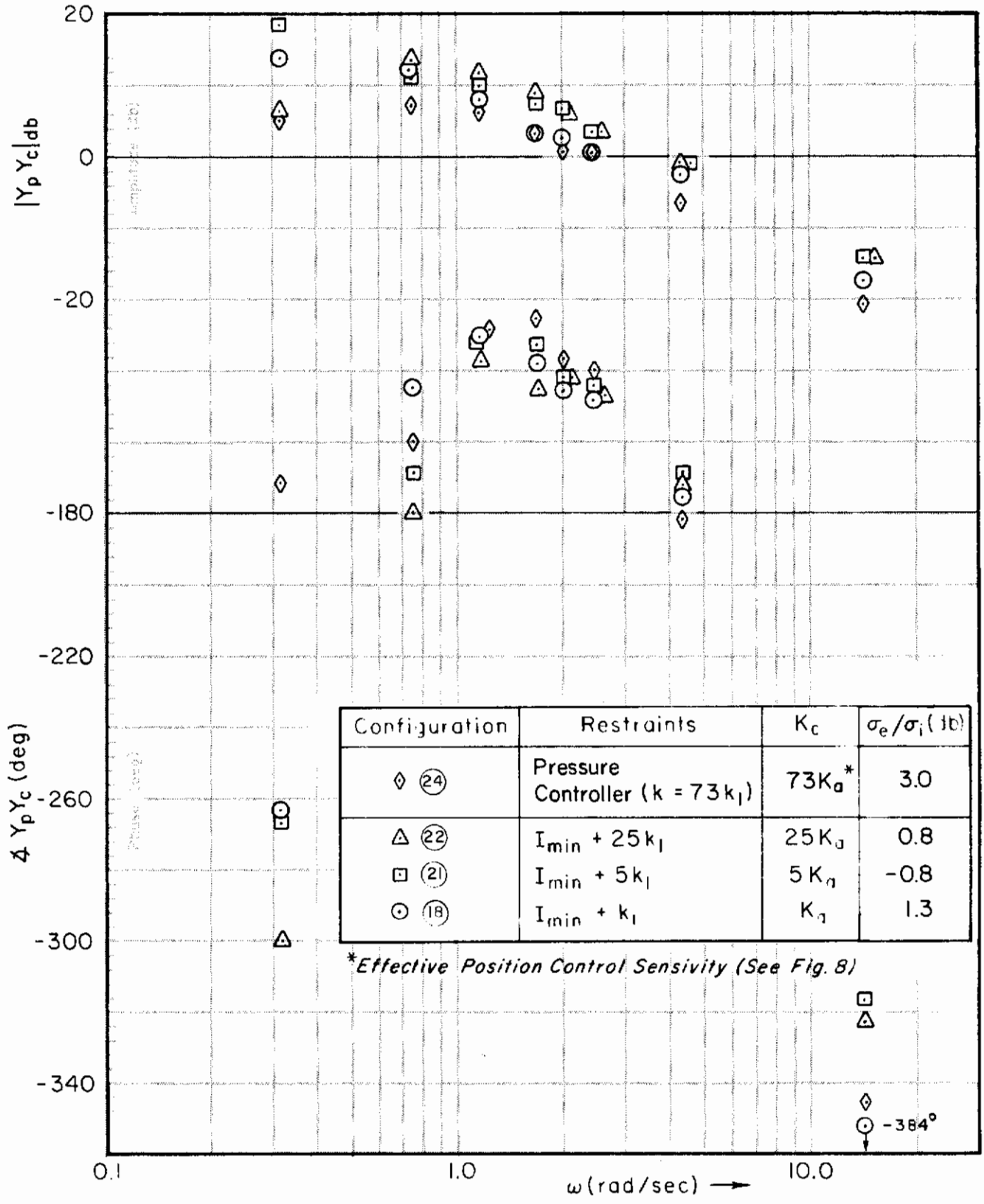

Configuration	Restraints	K_c	σ_e/σ_i (db)
◇ (24)	Pressure Controller ($k = 73k_1$)	$73K_a$*	3.0
△ (22)	$I_{min} + 25k_1$	$25K_a$	0.8
□ (21)	$I_{min} + 5k_1$	$5K_a$	-0.8
○ (18)	$I_{min} + k_1$	K_a	1.3

Figure 21. Averaged Open-Loop Describing Functions for $Y_c = K_c/s^2$ with Spring Rate and Control Sensitivity as Parameters

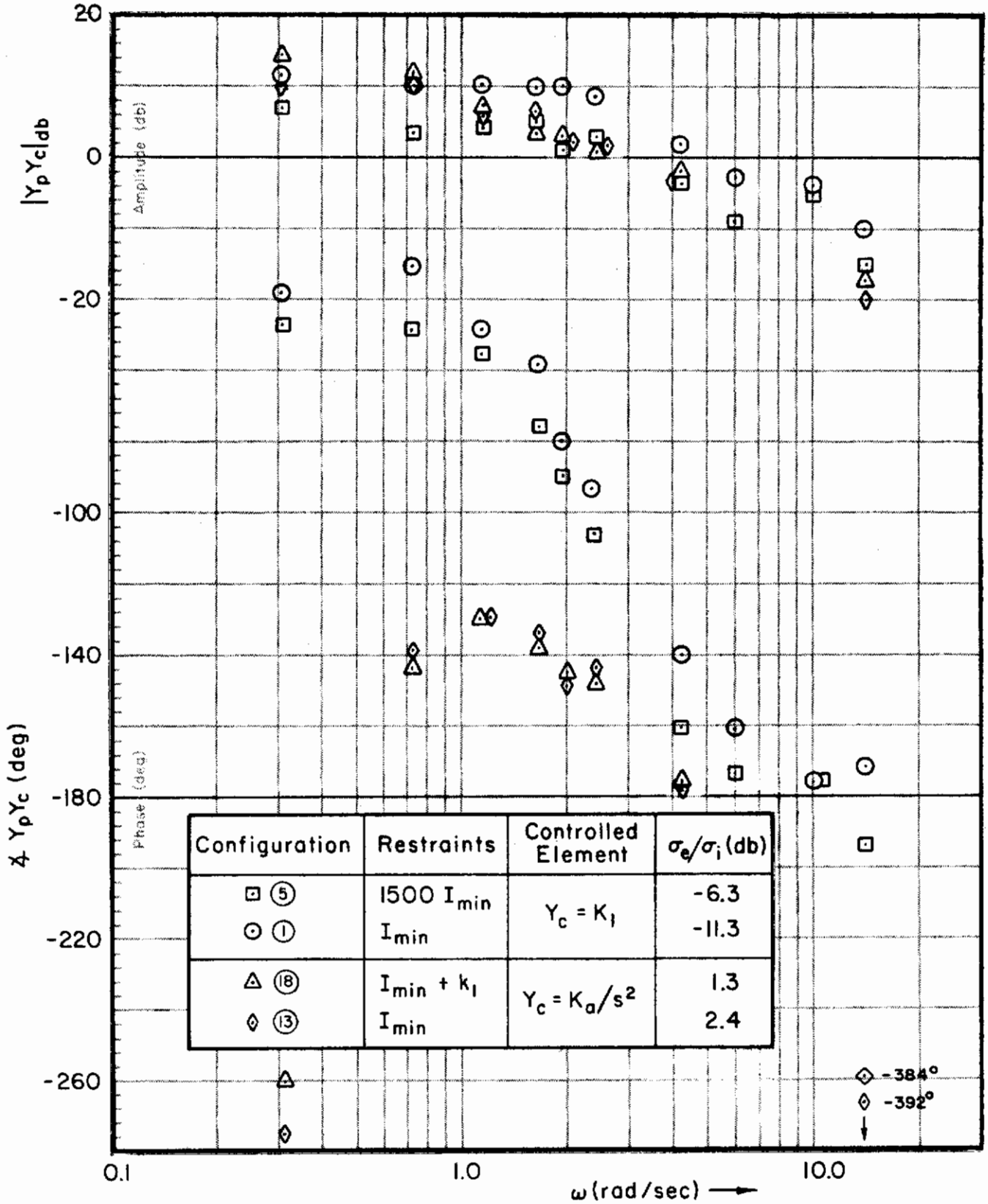

Figure 22. Averaged Open-Loop Describing Functions for the Effects of Dynamics Location

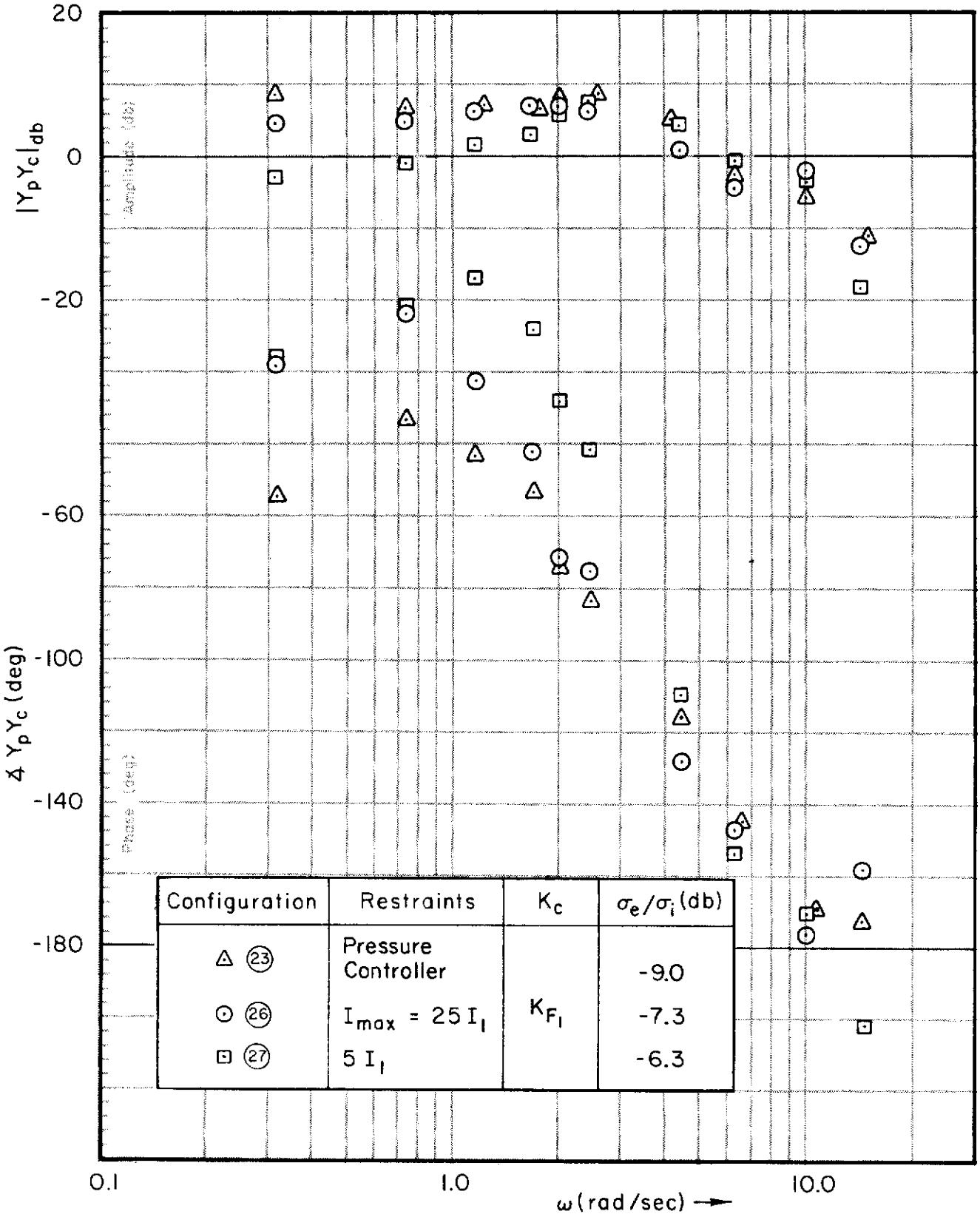

Figure 23. Averaged Open-Loop Describing Functions for $Y_c = K_c$, Force Control with Inertia as Parameter

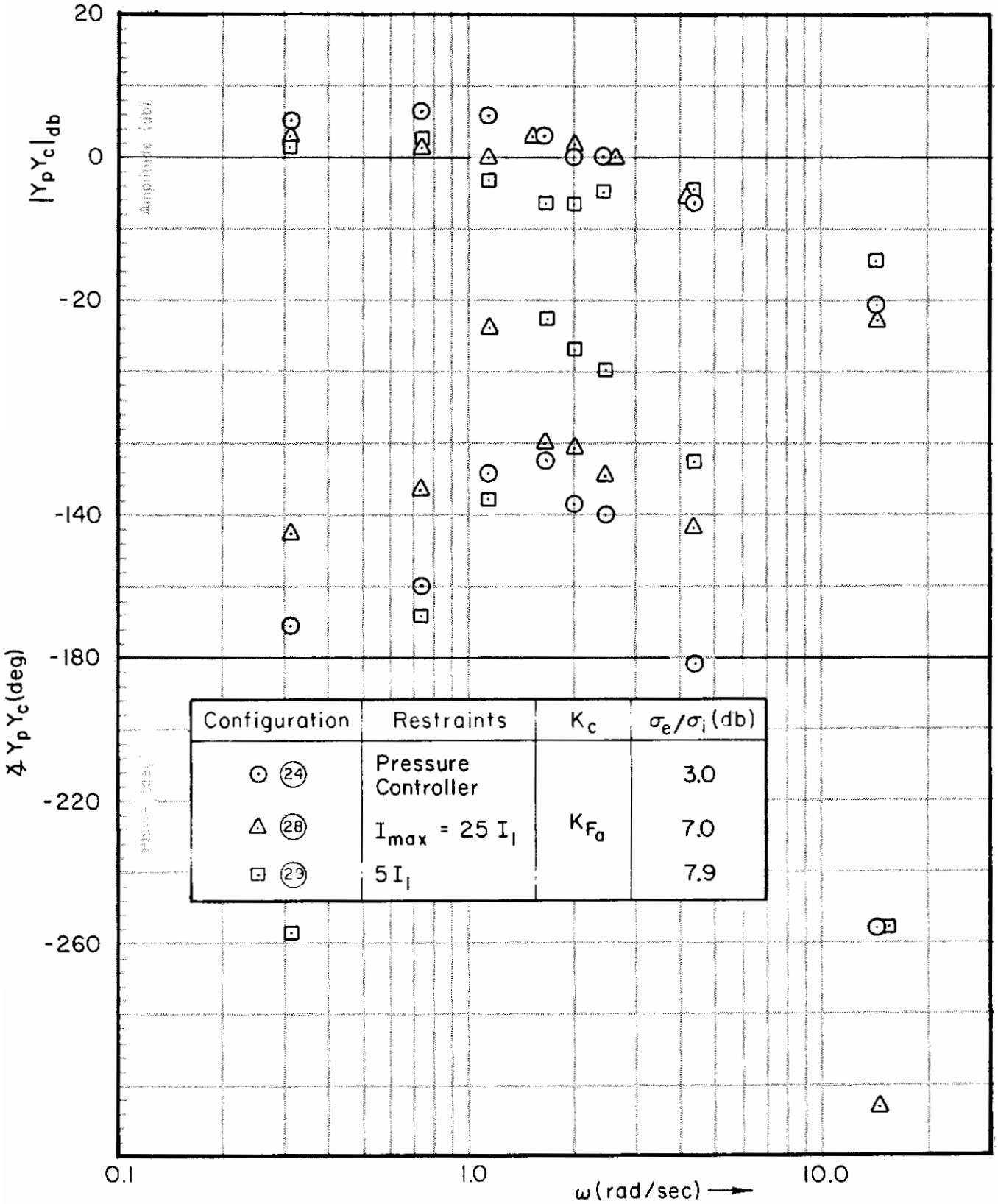

Figure 24. Averaged Open-Loop Describing Functions for $Y_c = K_c/s^2$, Force Control with Inertia as Parameter

SECTION V

CONCLUSIONS

This study, an exploratory investigation of the effects of load dynamics on human operator performance, provides inferential insight into the relative importance of limb position and output force senses in manual control. Conclusions relative to a large number of specific findings are given in the data interpretation in the text. The more general findings with respect to the five experimental objectives listed on page 24 are summarized below.

1. For spring restraints there was no practical difference in performance between the present pitch tracking experiments and those obtained from an earlier program for roll tracking.

2. Effects of manipulator restraints:

   a. For an "easy" controlled element ($Y_c = K_c$), performance was constant over a wide range of spring rates, while for a difficult controlled element ($Y_c = K_c/s^2$) performance was best at an intermediate spring rate.

   b. With no spring restraint, increasing the inertia above that contributed by the pilot's limb degrades performance considerably for both $Y_c = K_c$ and $Y_c = K_c/s^2$.

3. The pilot has nearly the same performance with the best pressure control configuration as with the best spring-restrained configuration.

4. For position control tasks the pilot can operate as a position output device, i.e., his describing function is appropriate for the controlled element. The force-displacement characteristics are largely swamped by a tight position feedback loop.

5. For $Y_c = K_c$ the human operator can control the force on an unrestrained very large inertia, effectively ignoring the extraneous position cues. System performance is little different than for the pressure controller. However, he is not as successful for $Y_c = K_c/s^2$; there is a large performance decrement from the pressure control configuration.

REFERENCES

1. McRuer, Duane, Dunstan Graham, Ezra Krendel, and William Reisener, Jr., Human Pilot Dynamics in Compensatory Systems: Theory, Models, and Experiments with Controlled Element and Forcing Function Variations, AFFDL-TR-65-15, July 1965.

2. Elkind, J. E., Characteristics of Simple Manual Control Systems, MIT Lincoln Lab. Tech. Rept. 111, 6 Apr. 1956.

3. Hall, I. A. M., Effects of Controlled Element on the Human Pilot, WADC-TR-57-509, Aug. 1958.

4. Notterman, J. M., and D. E. Page, Evaluation of Mathematically Equivalent Tracking Systems, Columbia Univ., Electronics Research Labs., Final Rept. F/135, 31 July 1960.

5. McRuer, Duane T., and Ezra S. Krendel, Dynamic Response of Human Operators, WADC-TR-56-524, Oct. 1957.

6. Krendel, Ezra S., and Duane T. McRuer, "A Servomechanisms Approach to Skill Development," J. Franklin Inst., Vol. 269, No. 1, Jan. 1960, pp. 24-42.

7. Vodovnik, L., C. Long, J. B. Reswick, A. Lippay, and D. Starbuck, "Myo-electric Control of Paralyzed Muscles," IEEE Trans., Vol. BME-12, No. 3-4, July-Oct. 1965, pp. 169-172.

8. McRuer, D. T., and R. E. Magdaleno, Human Pilot Dynamics with Various Manipulators, AFFDL-TR-66-138, Sept. 1966.

Unclassified
Security Classification

DOCUMENT CONTROL DATA - R&D
(Security classification of title, body of abstract and indexing annotation must be entered when the overall report is classified)

1. ORIGINATING ACTIVITY (Corporate author) Systems Technology, Inc. 13766 South Hawthorne Boulevard Hawthorne, California 90250	2a. REPORT SECURITY CLASSIFICATION Uncl. 2b. GROUP N/A

3. REPORT TITLE

EFFECTS OF MANIPULATOR RESTRAINTS ON HUMAN OPERATOR PERFORMANCE

4. DESCRIPTIVE NOTES (Type of report and inclusive dates)

Final Technical Report

5. AUTHOR(S) (Last name, first name, initial)

Magdaleno, R. E.
McRuer, D. T.

6. REPORT DATE	7a. TOTAL NO. OF PAGES	7b. NO. OF REFS
December 1966	47	7

8a. CONTRACT OR GRANT NO.	9a. ORIGINATOR'S REPORT NUMBER(S)
AF 33(657)-10835 b. PROJECT NO. 8219 c. Task: 821905 d.	AFFDL-TR-66-72 9b. OTHER REPORT NO(S) (Any other numbers that may be assigned this report) STI-TR-134-2

10. AVAILABILITY/LIMITATION NOTICES

Distribution of this document is unlimited.

11. SUPPLEMENTARY NOTES	12. SPONSORING MILITARY ACTIVITY
	AFFDL (FDCC) Wright-Patterson Air Force Base, Ohio 4543

13. ABSTRACT

This report is concerned with a series of experiments in which the effects of manipulator restraints, i.e., load dynamics imposed on the operator, are central. The purposes of this investigation are to:

a. Determine the load effects on the human operator's describing functions and performance measures for a representative variety of manipulator restraints and controlled elements.

b. Provide inferential insight into the relative importance of limb position and output force senses in manual control.

DD FORM 1 JAN 64 1473

Unclassified
Security Classification

14. KEY WORDS	LINK A		LINK B		LINK C	
	ROLE	WT	ROLE	WT	ROLE	WT
Human Response						
Manipulators						
Human Engineering						
Flight Control Systems						
Pilot Models						

INSTRUCTIONS

1. ORIGINATING ACTIVITY: Enter the name and address of the contractor, subcontractor, grantee, Department of Defense activity or other organization *(corporate author)* issuing the report.

2a. REPORT SECURITY CLASSIFICATION: Enter the overall security classification of the report. Indicate whether "Restricted Data" is included. Marking is to be in accordance with appropriate security regulations.

2b. GROUP: Automatic downgrading is specified in DoD Directive 5200.10 and Armed Forces Industrial Manual. Enter the group number. Also, when applicable, show that optional markings have been used for Group 3 and Group 4 as authorized.

3. REPORT TITLE: Enter the complete report title in all capital letters. Titles in all cases should be unclassified. If a meaningful title cannot be selected without classification, show title classification in all capitals in parenthesis immediately following the title.

4. DESCRIPTIVE NOTES: If appropriate, enter the type of report, e.g., interim, progress, summary, annual, or final. Give the inclusive dates when a specific reporting period is covered.

5. AUTHOR(S): Enter the name(s) of author(s) as shown on or in the report. Enter last name, first name, middle initial. If military, show rank and branch of service. The name of the principal author is an absolute minimum requirement.

6. REPORT DATE: Enter the date of the report as day, month, year; or month, year. If more than one date appears on the report, use date of publication.

7a. TOTAL NUMBER OF PAGES: The total page count should follow normal pagination procedures, i.e., enter the number of pages containing information.

7b. NUMBER OF REFERENCES: Enter the total number of references cited in the report.

8a. CONTRACT OR GRANT NUMBER: If appropriate, enter the applicable number of the contract or grant under which the report was written.

8b, 8c, & 8d. PROJECT NUMBER: Enter the appropriate military department identification, such as project number, subproject number, system numbers, task number, etc.

9a. ORIGINATOR'S REPORT NUMBER(S): Enter the official report number by which the document will be identified and controlled by the originating activity. This number must be unique to this report.

9b. OTHER REPORT NUMBER(S): If the report has been assigned any other report numbers *(either by the originator or by the sponsor)*, also enter this number(s).

10. AVAILABILITY/LIMITATION NOTICES: Enter any limitations on further dissemination of the report, other than those imposed by security classification, using standard statements such as:

(1) "Qualified requesters may obtain copies of this report from DDC."

(2) "Foreign announcement and dissemination of this report by DDC is not authorized."

(3) "U. S. Government agencies may obtain copies of this report directly from DDC. Other qualified DDC users shall request through _____."

(4) "U. S. military agencies may obtain copies of this report directly from DDC. Other qualified users shall request through _____."

(5) "All distribution of this report is controlled. Qualified DDC users shall request through _____."

If the report has been furnished to the Office of Technical Services, Department of Commerce, for sale to the public, indicate this fact and enter the price, if known.

11. SUPPLEMENTARY NOTES: Use for additional explanatory notes.

12. SPONSORING MILITARY ACTIVITY: Enter the name of the departmental project office or laboratory sponsoring *(paying for)* the research and development. Include address.

13. ABSTRACT: Enter an abstract giving a brief and factual summary of the document indicative of the report, even though it may also appear elsewhere in the body of the technical report. If additional space is required, a continuation sheet shall be attached.

It is highly desirable that the abstract of classified reports be unclassified. Each paragraph of the abstract shall end with an indication of the military security classification of the information in the paragraph, represented as *(TS), (S), (C), or (U)*.

There is no limitation on the length of the abstract. However, the suggested length is from 150 to 225 words.

14. KEY WORDS: Key words are technically meaningful terms or short phrases that characterize a report and may be used as index entries for cataloging the report. Key words must be selected so that no security classification is required. Identifiers, such as equipment model designation, trade name, military project code name, geographic location, may be used as key words but will be followed by an indication of technical context. The assignment of links, rules, and weights is optional.